

NPS-61Bs77061

# NAVAL POSTGRADUATE SCHOOL

## Monterey, California



INVESTIGATION OF GIANT MULTIPOLE RESONANCES  
IN MEDIUM AND HEAVY NUCLEI  
BY INELASTIC ELECTRON SCATTERING

Fred R. Buskirk

Final Technical Report  
Project PHY 73 21573  
(15 Oct 1974 to 31 Oct 1976)

Sponsor: National Science Foundation

Approved for public release; distribution unlimited.

NAVAL POSTGRADUATE SCHOOL  
Monterey, California

Rear Admiral Isham W. Linder  
Superintendent

Jack R. Borsting  
Provost

The work reported herein was supported by the National Science Foundation.

Reproduction of all or part of this report is authorized.

This report was prepared by:

## UNCLASSIFIED

SECURITY CLASSIFICATION OF THIS PAGE (When Data Entered)

REPORT DOCUMENTATION PAGE		READ INSTRUCTIONS BEFORE COMPLETING FORM
1. REPORT NUMBER NPS-61Bs77061	2. GOVT ACCESSION NO.	3. RECIPIENT'S CATALOG NUMBER
4. TITLE (and Subtitle) Investigation of Giant Multipole Resonances in Medium and Heavy Nuclei by Inelastic Electron Scattering.		5. TYPE OF REPORT & PERIOD COVERED Final Technical Report
7. AUTHOR(s) Fred R. Buskirk		6. PERFORMING ORG. REPORT NUMBER PHY 73 21573 and PHY 73 21573 A01
9. PERFORMING ORGANIZATION NAME AND ADDRESS Naval Postgraduate School Monterey, CA 93940		10. PROGRAM ELEMENT, PROJECT, TASK AREA & WORK UNIT NUMBERS
11. CONTROLLING OFFICE NAME AND ADDRESS The National Science Foundation Washington, D.C. 20550		12. REPORT DATE MAY 1977
14. MONITORING AGENCY NAME & ADDRESS(if different from Controlling Office)		13. NUMBER OF PAGES UNCLASSIFIED
16. DISTRIBUTION STATEMENT (of this Report)  Approved for public release; distribution unlimited.		15. SECURITY CLASS. (of this report) UNCLASSIFIED
17. DISTRIBUTION STATEMENT (of the abstract entered in Block 20, if different from Report)		
18. SUPPLEMENTARY NOTES		
19. KEY WORDS (Continue on reverse side if necessary and identify by block number) Electron Scattering Giant Resonances Lead, Gold, Holmium, Yttrium, Nickel		
20. ABSTRACT (Continue on reverse side if necessary and identify by block number) Giant Resonance Measurements in Medium and Heavy Nuclei by Inelastic Electron Scattering using the Naval Postgraduate School 120 MeV LINAC, included the nuclei $^{208}\text{Pb}$ , $^{197}\text{Au}$ , $^{165}\text{Ho}$ , $^{60}\text{Ni}$ and $^{89}\text{Y}$ ; investigations of the radiation tail and of the giant resonance line shape. (Cont'd)		

## UNCLASSIFIED

SECURITY CLASSIFICATION OF THIS PAGE(When Data Entered)

## 20. ABSTRACT (Cont'd)

One question which arose from earlier experiments and which has excited much interest concerns the monopole mode which we reported to be at  $53 A^{-1/3}$  MeV, 8.9 MeV in  $^{208}\text{Pb}$ . Using improved techniques, we re-evaluated our existing data. The giant resonance region was resolved in fine structure (less than 500 KeV) and resonance structure (wider than 1800 KeV). The fine structure around 10.5 MeV as well as the broad resonance (10.8 MeV) were all found to have an E2 angular distribution, and assumption of  $\Delta T = 1$  for the fine structure, contrasted to  $\Delta T = 0$  for the broad resonance explains many of the apparent contradictions. The broad 8.9 MeV resonance which might be E2 or E0 from the angular distribution, is more likely to be E0, based on sum rule and other arguments.

Some of the important results for  $^{165}\text{Ho}$  included the split giant dipole state as seen in  $(\gamma, n)$  and broadening for the isoscalar quadrupole mode expected in a deformed nucleus. The isovector quadrupole mode was observed for the first time to be split. No broadening was seen for the  $53 A^{-1/3}$  state, which is in accord with the monopole assignment for  $^{208}\text{Pb}^*$ .

For  $^{89}\text{Y}$ , an E3 state at 13.5 MeV was found which may be  $1 \text{ h}\omega \Delta T = 1$  excitation (where  $\text{h}\omega$  = shell spacing), but no evidence is found for E3 strength; the latter is seen for heavy nuclei. No excess cross section was found near the giant dipole resonance; this strength would appear if the state were at the energy  $80 A^{-1/3}$  MeV proposed recently.

We investigated  $^{58}\text{Ni}$  and  $^{60}\text{Ni}$ , but only the latter in the period covered by this report. We will give a complete account in a later report.

UNCLASSIFIED

SECURITY CLASSIFICATION OF THIS PAGE(When Data Entered)

NAVAL POSTGRADUATE SCHOOL  
Monterey, California

FINAL TECHNICAL REPORT

Sponsor : The National Science Foundation

Title : Investigation of Giant Multipole Resonances in Medium and Heavy Nuclei by Inelastic Electron Scattering

Grant Number : PHY 73 21573 and PHY 74 21573 A01

Period of Research : 15 October 1974 to 31 October 1976

Principal Investigator:

Description of Research:

A. Introduction

This report covers the research done from October 1974 to October 1976 on Giant Resonances in Medium and Heavy Nuclei by Inelastic Electron Scattering, using the Naval Postgraduate School 120 MeV Linac. These experiments include the nuclei  $^{208}\text{Pb}$ ,  $^{197}\text{Au}$ ,  $^{165}\text{Ho}$ ,  $^{60}\text{Ni}$ , and  $^{89}\text{Y}$ . For details we refer to the theses and publications which have resulted from these experiments while some of the important results are summarized. Other activities included investigations of the radiation tail and of the giant resonance line shape, which are essential to fitting the ( $e,e'$ ) spectra, and significant improvements of the Linac.

B. Experiments with  $^{197}\text{Au}$  and  $^{208}\text{Pb}$

The experiments done before this report period were published in PRL in December 1974. The isoscalar quadrupole resonance was seen at  $60 \text{ A}^{-1/3}$  MeV as expected. New results included evidence for a monopole assignment (E0) at  $53 \text{ A}^{-1/3}$  MeV, one of the earliest reports for the isovector quadrupole mode at  $133 \text{ A}^{-1/3}$  MeV and observation of E3 strength at  $105 \text{ A}^{-1/3}$  MeV. Strengths for all the above were given (see Publication 1).

One question which has excited much interest concerns the monopole mode which we reported to be at  $53 \text{ A}^{-1/3}$  MeV, 8.9 MeV in Pb. The angular distribution in ( $e,e'$ ) is the same for E0 and E2, which makes direct identification difficult.

While considering the possibility for new experiments on  $^{208}\text{Pb}$  to either confirm or refute the existence of the monopole state at  $53 \text{ A}^{-1/3}$  MeV, we realized that before launching into new experiments, much could be learned

from a new evaluation of our existing data (see Publication 4). With our improved spectrum analysis program we made an analysis consistent with  $(\alpha, \alpha')$  and with  $(\gamma, n)$  experiments. The giant resonance region was resolved in line structure (less than 500 KeV) and resonance structure (wider than 1800 KeV). The fine structure around 10.5 MeV as well as the broad resonance (10.8 MeV) were all found to have an E2 angular distribution, and assumption of  $\Delta T = 1$  for the fine structure, contrasted to  $\Delta T = 0$  for the broad resonance, explains many of the apparent contradictions. Fine structure at 8.9 MeV could not be identified, but the broad 8.9 MeV resonance, which might be E2 or E0 from the angular distribution, is more likely to be E0. An E2 assignment for this state would lead to a total observed isoscalar E2 strength of 148% of the energy weighted sum rule, which is much too large. This sum rule argument then provides the most solid evidence that the 8.9 MeV resonance in  $^{208}\text{Pb}$  is the E0 breathing mode. In addition, a second isoscalar E2 mode as a general feature of heavy nuclei seems to be quite unlikely, that is not predicted by theory and very difficult to explain (see Publications 1,4).

#### C. Holmium ( $^{165}\text{Ho}$ )

The holmium  $(e, e')$  experiments were performed at  $75^\circ$  and various incident energies to vary the momentum transfer. The range of excitation energy, 5 to 40 MeV, was larger than in previous experiments. Some of the important results included the split giant dipole state as seen in  $(\gamma, n)^1$  and broadening of the isoscalar quadrupole mode as expected in a deformed nucleus. The isovector quadrupole mode was observed for the first time to be split. Finally, no broadening was seen for the  $53 \text{ A}^{-1/3}$  MeV state, which is in accord with the monopole assignment made in the Pb experiments (see Publication 2).

#### D. Yttrium ( $^{89}\text{Y}$ )

These experiments were performed as a general extension of our previous work on  $^{208}\text{Pb}$ ,  $^{197}\text{Au}$ , and  $^{165}\text{Ho}$  to lighter nuclei. Also, more specifically, we wished to check the conclusion<sup>2</sup> for  $^{90}\text{Zr}$  that the quadrupole resonance is broader than the giant dipole state. This result is not true for heavy nuclei.

Some of the main conclusions for  $^{89}\text{Y}$  are (see Publication 5):

1. The isovector E2 strength can be 40% to 75% of the energy weighted sum rule, depending on the total width  $\Gamma$  assumed.
2. An E3 state at 13.5 MeV is found which may be  $1 \hbar\omega \Delta T = 1$  excitation (where  $\hbar\omega$  = shell spacing), but no evidence is found for E3  $3 \hbar\omega$  strength; the latter is seen for heavy nuclei.
3. No excess cross section is found near the giant dipole resonance; this strength would appear if the E0 state were at the energy  $80 A^{-1/3}$  MeV proposed recently<sup>3</sup>.

#### E. Nickel ( $^{58}\text{Ni}$ and $^{60}\text{Ni}$ )

We investigated  $^{58}\text{Ni}$  and  $^{60}\text{Ni}$  under identical conditions, but only the latter in the period covered by this report. We will give a complete account in a later report. One striking result concerns the giant dipole resonance, which in  $(\gamma, n)$  experiments<sup>4</sup> is much smaller for  $^{58}\text{Ni}$  compared to  $^{60}\text{Ni}$ . Our experiments, which measure the total E1 strength, not just the  $(\gamma, n)$  channel, show precisely the opposite result, namely that  $^{58}\text{Ni}$  has a larger E1 strength. If  $(e, e')$  and  $(\gamma, n)$  results are to be reconciled, either the  $(\gamma, p)$  experiments are wrong or some other channel, possibly  $(\gamma, D)$  must be present and large in  $^{58}\text{Ni}$ , but small in  $^{60}\text{Ni}$ .

#### F. Improvements in the Linac and Spectrum Analysis: (Publication 3)

A major Linac improvement was undertaken in 1975. The vacuum system was completely rebuilt and the result has been much more reliable operation. Problems in the electroexcitation of giant resonances have always been associated with the large underlying radiation tail and the overlapping resonance structure. We have made advances in both areas, which increases the possibility of extracting resonance parameters for weak resonances even at excitation energies as high as 20 to 40 MeV.

The radiation tail calculation now used in our analyses accounts for virtually all the radiative background, and has been demonstrated to fit observed spectra over a wide range of excitation energy for nuclei between  $^{58}\text{Ni}$  and  $^{208}\text{Pb}$  (see Publication 5).

The investigation of the line shape had to be undertaken, because the choice of a certain line shape greatly influences the cross section extracted for weak resonances close to overlapping strong resonances. For example, the 9 MeV resonance in  $^{197}\text{Au}$  and the  $^{208}\text{Pb}$ , for which we have given evidence for an E0 assignment, is difficult to resolve from the nearby isoscalar E2 quadrupole resonance. Analysis of ( $\gamma$ ,n) measurements with monochromatic photons showed clearly that the dependence of the reduced transition probability,  $B(E1)$ , on excitation energy follows a symmetric Breit-Wigner shape, although a Lorentz form describes the resulting cross section (see Publication 3).

#### REFERENCES

1. B. L. Berman, M. A. Kelly, R. L. Bramblett, J. T. Caldwell, H. S. Davis, and S. C. Fultz; Phys. Rev. 185, 1576 (1969).
2. S. Fukuda and Y. Torizuka; Phys. Rev. Lett. 29, 1109 (1972).
3. M. N. Harakeh, K. van der Borg, T. I. Shimatsu, H. P. Morsch, A. van der Woude, and F. E. Bertrand; Phys. Rev. Lett. 38, 676 (1977).
4. S. C. Fultz, R. A. Alvarez, B. L. Berman, and P. Meyer; Phys. Rev. C10, 608 (1974).

## PUBLICATIONS

### Published Papers:

1. Electroexcitation of Giant Multipole Resonances in  $^{197}\text{Au}$  and  $^{208}\text{Pb}$  between 5 and 40 MeV Excitation Energy with 90 MeV Electron  
R. Pitthan, F. R. Buskirk, E. B. Dally, J. N. Dyer, and  
X. K. Maruyama  
*Phys. Rev. Lett.* 33, 849 (1974)
2. The Width of the E2 ( $\Delta T = 0$  and  $\Delta T = 1$ ) Giant Resonances in  $^{165}\text{Ho}$   
G. L. Moore, F. R. Buskirk, E. B. Dally, J. N. Dyer,  
X. K. Maruyama, and R. Pitthan  
*Z. Naturforsch* 31a, 668 (1976)

### Papers Submitted (Preprints enclosed)

3. The Natural Line Shape of the Giant Dipole Resonance  
E. F. Gordon and R. Pitthan  
Accepted for publication in *Nucl. Instr. Methods*
4. The Isospin of the Fine Structure between 8 and 12 MeV in  $^{208}\text{Pb}$  and its Implication for the Multipole Assignment of the 8.9 MeV Resonance  
R. Pitthan and F. R. Buskirk  
Submitted to *Phys. Rev. C*
5. Giant Resonances and Bound Collective States Observed in the Scattering of 92.5 MeV Electrons from the Closed Neutron Shell Nucleus  $^{89}\text{Y}$  between Excitation Energies from 2 to 55 MeV  
R. Pitthan, F. R. Buskirk, E. B. Dally, J. O. Shannon,  
and W. H. Smith  
Submitted to *Phys. Rev. C*

THESES

1. G. L. Moore, "Electroexcitation of Giant Resonances Between 5 and 30 MeV Excitation Energy in  $^{165}\text{Ho}$ " (December 1974).
2. E. F. Gordon, "An Investigation of the Natural Line Shape of the Giant Dipole Resonance" (December 1975).
3. D. H. Dubois II and G. M. Bates, "Electroexcitation of Giant Resonances in  $^{60}\text{Ni}$  Between 5 MeV and 30 MeV Excitation Energy" (June 1976).
4. J. O. Shannon and W. H. Smith, "Electroexcitation of Giant Resonances Between 5.1 MeV and 38 MeV Excitation Energy in  $^{89}\text{Y}$ " (June 1976).

## SCIENTIFIC COLLABORATORS

Rainer Pitthan has been supported exclusively by N.S.F. funds, and conversely, the N.S.F. funds have been used exclusively for his support.

J. N. Dyer, X. K. Maruyama, and E. B. Dally, while not supported by the N.S.F. funds, have contributed to the giant resonance research.

## COMMENTS

We believe that further work should be done on giant resonances by  $(e, e')$ . Our present survey of nuclei should be extended to lighter elements and other isotope comparisons. A very illuminating example is provided by our  $^{58}\text{Ni}$  and  $^{60}\text{Ni}$  experiment which reveals new information about the strength of the one resonance (the giant dipole) which is supposed to be so well understood from  $(\gamma, n)$  experiments.

The versatility of the  $(e, e')$  measurements rests on two characteristics, namely the momentum transfer may be varied independently from excitation energy, and the total electromagnetic interaction cross section is measured. These two features mean that our type of experiments form a needed complement to  $(\gamma, n)$  and  $(e, e')$  coincidence experiments.

Fred R. Buskirk  
Professor of Physics  
Naval Postgraduate School  
Monterey, California 93940

## APPENDIX

The five publications follow.

# Electroexcitation of Giant Multipole Resonances in $^{197}\text{Au}$ and $^{208}\text{Pb}$ between 5 and 40 MeV Excitation Energy with 90-MeV Electrons\*

R. Pitthan, † F. R. Buskirk, E. B. Dally, J. N. Dyer, and X. K. Maruyama  
*Naval Postgraduate School, Monterey, California 93940*  
 (Received 29 July 1974)

Inelastic electron scattering with 90-MeV electrons shows previously observed giant resonances at excitation energies of  $63A^{-1/3}$  ( $E_2$ ),  $81A^{-1/3}$  ( $E_1$ ),  $105A^{-1/3}$  ( $E_3$ ), and  $130A^{-1/3}$  MeV ( $E_2$ ). Distorted-wave-Born-approximation analysis of additional structure at  $53A^{-1/3}$  and  $195A^{-1/3}$  MeV suggests a monopole assignment. Transverse contributions to the  $E_1$  matrix element are compatible with an electric spin-flip. Differing widths of the respective resonances in the two nuclei are explained through dynamic deformation of Au. The reduced electric transition strengths  $B(EL)$  are given.

Ever since Goldhaber and Teller explained the giant dipole resonance as a collective oscillation of neutrons against protons,<sup>1</sup> extensions of their model have raised the question of the existence of giant resonances with other multipolarities, especially those with quadrupole and monopole characters.<sup>2</sup> The first experimental evidence of a giant quadrupole resonance several MeV below the giant dipole resonance was found in  $(e, e')$  experiments at Darmstadt University.<sup>3</sup> This was soon corroborated in the reevaluation of  $(p, p')$  data<sup>4</sup> at Oak Ridge National Laboratory.<sup>5</sup> The results were based on a model by Satchler.<sup>6</sup> Additional evidence was found in  $(e, e')$  experiments at Sendai University.<sup>7</sup> Especially significant is the  $(e, e')$  experiment of the latter group on  $^{208}\text{Pb}$ ,<sup>8</sup> which not only showed a splitting of the "new" resonance in this nucleus into at least three states,<sup>9</sup> but furthermore found two other resonances at 19 MeV ( $E_3$ ) and 22 MeV ( $E_2$ ). Each of these three resonances satisfies a large fraction of the appropriate sum rule, indicating that real giant resonances were observed. The lower  $E_2$  resonance  $E_x = 63A^{-1/3}$  MeV is generally referred to as the isoscalar ( $\Delta T = 0$ ) and the higher resonance at  $E_x = 130A^{-1/3}$  MeV as the isovector ( $\Delta T = 1$ ) branch of the giant quadrupole resonance.<sup>10</sup> Several experiments with various particles<sup>11</sup> have confirmed, more or less, the picture sketched above. No experimental evidence has been reported so far concerning the isoscalar and isovector monopole resonances.

The experiments reported were carried out with 90-MeV incident electrons and an overall resolution of 500 keV at the linear accelerator laboratory of the Naval Postgraduate School.<sup>12</sup> Comparison of the scattered electron spectra from  $^{197}\text{Au}$  and  $^{208}\text{Pb}$  in Figs. 1 and 2 reveals striking differences throughout the covered excitation range. The line-shape fitting procedure

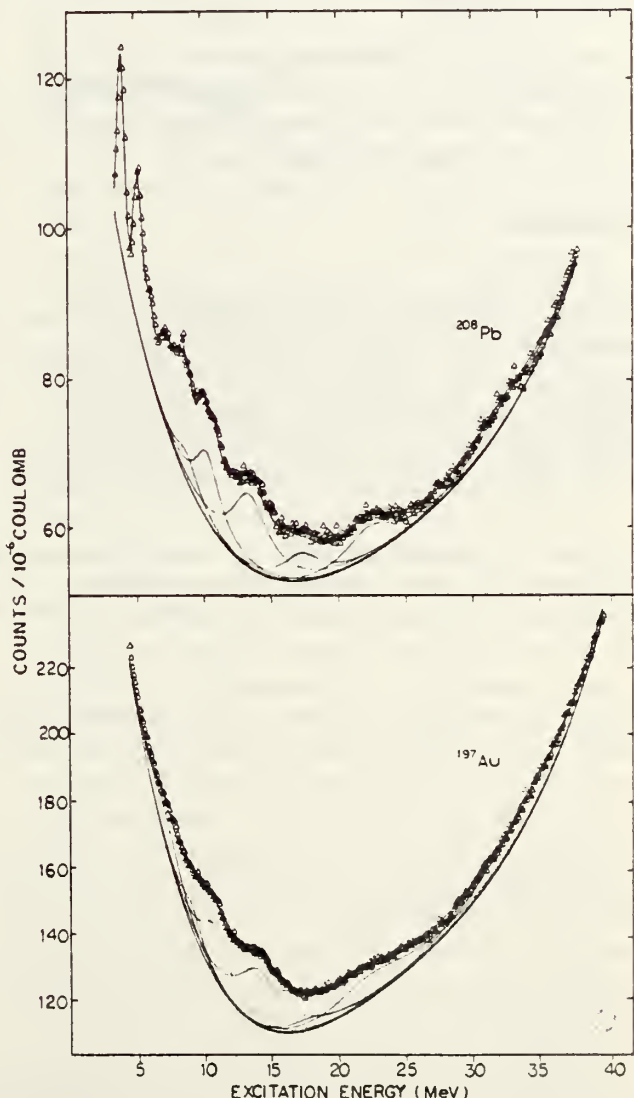


FIG. 1. Spectrum of 90-MeV electrons, scattered inelastically from Pb and Au. The fitted background which consists of the radiation tail and the machine background is shown. The counting rate is corrected for the constant momentum dispersion of the spectrometer. Thus the error increases with the excitation energy.

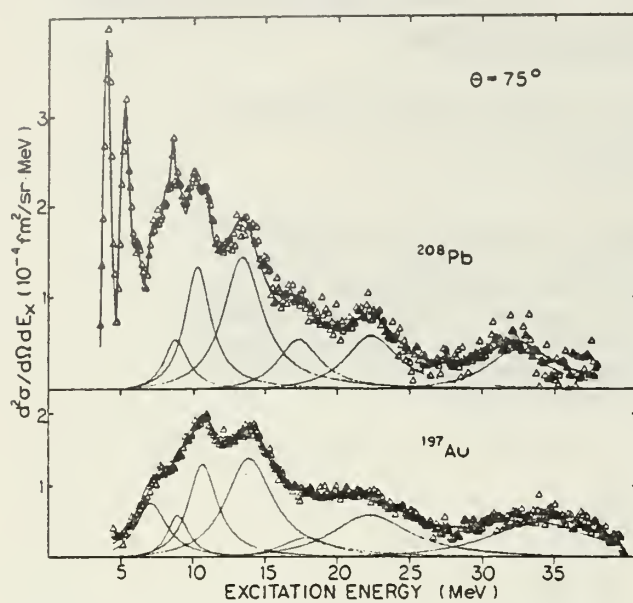


FIG. 2. Same as Fig. 1, after subtraction of the fitted background.

described by Pittman<sup>13</sup> and the radiative-tail calculation described in Ref. 9 were used. The resonances shown in the Au spectrum are those required to consistently fit the measurements with 90-MeV incident electrons at angles of 60°, 75°, 90°, 105°, and 120°. The Pb spectrum was

fitted by the resonances shown as well as the states which are known and have a natural width of less than 500 keV.

The difference in structure above 12 MeV can be explained by the dynamic collective model.<sup>14</sup> Although the ground state of Au is almost spherical, the giant dipole resonance at 14 MeV is much wider than in Pb. This broadening is due to an unresolved splitting,<sup>15</sup> indicating a dynamic deformation of the Au nucleus. The deformation becomes greater with higher excitation energy and leads to a greater fragmentation of strength among the different vibrational axes. It was possible to decompose each of the resonances at 18, 23, and 33 MeV in Au into two Breit-Wigner resonances. However, because of our method of fitting the background simultaneously with the resonances, the extraction of the cross sections became unreliable, so the results quoted here are obtained assuming one wide Breit-Wigner curve per resonance only.

Our experiment agrees with what is known for the 11-<sup>9</sup> and 22-MeV resonances.<sup>8,16</sup> We will therefore deal only with the other resonances. A more detailed account of all the results will be given elsewhere.<sup>17</sup> The final results for both nuclei as extracted from the 75° measurements are listed in Table I.

TABLE I. Comparison of results for Au and Pb as extracted from the 75° measurements. Columns 2 and 3 show multipolarity and isospin assignments assumed.

			197 Au							208 Pb						
E <sub>x</sub> [A <sup>-1/3</sup> MeV]	EL	ΔT	E <sub>x</sub> [MeV]	B(EL) [fm <sup>2L</sup> ] <sup>a</sup>	Γ <sub>nat</sub> [MeV]	EWSR <sup>b</sup> [%]	SPU <sup>c</sup>	Others B(EL)	E <sub>x</sub> [MeV]	B(EL) [fm <sup>2L</sup> ] <sup>a</sup>	Γ <sub>nat</sub> [MeV]	EWSR <sup>b</sup> [%]	SPU <sup>c</sup>	Others B(EL)		
53	E0	0	9.2	(3.6±1.8)10 <sup>3</sup>	2.2±0.5	35	--	--	8.9	(5±3)10 <sup>3</sup>	1.8±0.5	50	--	--		
63	E2	0	10.8	(5.2±1.2)10 <sup>3</sup>	2.9±0.2	77	15.5	(8.4±1.6)10 <sup>3</sup> <sup>h</sup> )	10.5	(6.7±2.5)10 <sup>3</sup>	2.8±0.3	95	21.5	(2.6±0.9)10 <sup>3</sup> <sup>f</sup> ) (2.6±0.3)10 <sup>3</sup> <sup>g</sup> )		
81	E1	1	14.0	100±20 <sup>d</sup> 50±10 <sup>e</sup>	4.5±0.2	200	15.0	82±11 <sup>d</sup> h)	13.6	103±20 53±10	3.9±0.1	205	16	64±8 <sup>d</sup> f) 71±5 <sup>i</sup> )		
105	E3	0	18.0	(1.7±0.8)10 <sup>5</sup>	5.2±0.7	45	10.0	--	17.5	(3.2±1.5)10 <sup>5</sup>	4.2±0.7	90	17	(1.8±0.6) <sup>g</sup>		
105		1				30						60			(-1.6)	
133	E2	1	23.0	(4.6±1.5)10 <sup>3</sup>	7±1	95	13.5	(6.5±1.4)10 <sup>3</sup> <sup>h</sup> )	22.5	(4.2±1.4)10 <sup>3</sup>	5±1	85	14	(3.4±1)10 <sup>3</sup> <sup>g</sup> )		
195	E0	1	33.5	(10±3)10 <sup>3</sup>	10.5±2	250	--	--	33.0	(6.5±3)10 <sup>3</sup>	6±1	150	--	--		

<sup>a</sup>For the monopole  $|M_{if}|^2$  (fm<sup>4</sup>).

<sup>b</sup>Energy-weighted sum rule Ref. 19.

<sup>c</sup>Single particle units Ref. 20.

<sup>d</sup>Surface oscillation  $\rho_{tr}(r) \sim d\rho_0(r)/dr$ .

<sup>e</sup>Volume oscillation  $\rho_{tr}(r) \sim \rho_0(r)$ .

<sup>f</sup>Ref. 9.

<sup>g</sup>Ref. 8.

<sup>h</sup>Ref. 15.

<sup>i</sup>Ref. 14.

<sup>k</sup>Extracted from a 2-MeV-wide range only.

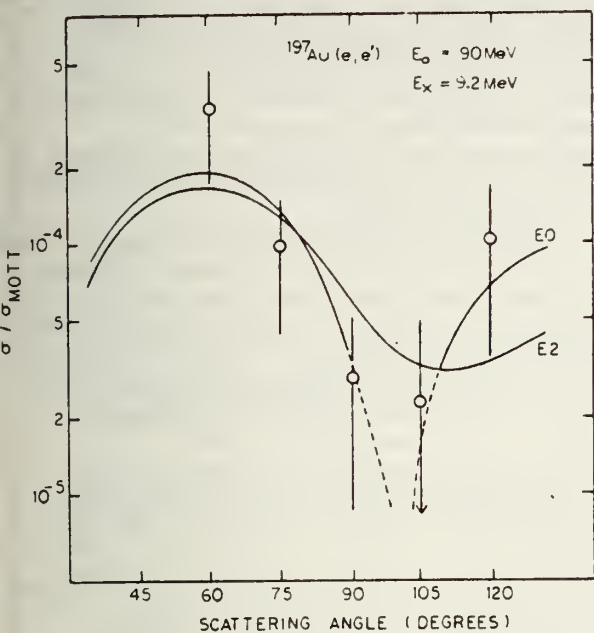


FIG. 3. Ratio of the inelastic cross section of the resonance at 9.2 MeV to the Mott cross section as a function of scattering angle. The curves show the results of DWBA calculations assuming an  $E_0$  or an  $E_2$  assignment. At  $105^\circ$  we did not see a resonance. The open circle corresponds to a resonance with a height of 1 standard deviation in the count rate and is, therefore, regarded as an upper limit. The error at  $105^\circ$  represents 1 additional standard deviation.

In Fig. 3 the ratio of the integrated cross section divided by the Mott cross section, which defines the square of the form factor, is shown for the resonance at 9.2 MeV ( $= 53A^{-1/3}$  MeV) and is compared to distorted-wave Born-approximation (DWBA) calculations. While for small scattering angles (low momentum transfer)  $E_0$  and  $E_2$  have the same angular dependence, they are different at the second maximum. There are, however, computational problems connected with the minimum, indicated by the dotted lines. This experiment is, nevertheless, the first experimental indication for the monopole giant resonance, and is a consequence one can obtain the value of the nuclear compressibility.<sup>2</sup> The evaluation was based on the usual DWBA code,<sup>18</sup> which was changed for the breathing mode as described by Kassis.<sup>19</sup>

An  $E_0$  resonance at  $E_r = 53A^{-1/3}$  MeV would agree with experimental results in  $N = 82$  nuclei, in which a resonance of  $E_0$  or  $E_2$  character was found.<sup>13</sup> Stronger support comes from comparison of  $(e, e')$  and  $(\gamma, n)$  experiments in Pb where the triplet of states at 10.2, 10.6, and 11.2 MeV

is identified as being  $E_2$  or  $E_0$  on the basis of the angular distribution.<sup>8,9</sup> However, the  $E_0$  assignment is ruled out by noting<sup>9</sup> that the fine structure in the  $(\gamma, n)$  spectra<sup>15</sup> may be explained only if an  $E_2$  transition is assumed. In contrast, the resonance at 8.85 MeV has the same angular distribution as the 10.6-MeV triplet, implying either an  $E_2$  or  $E_0$  assignment, but no line is seen in the  $(\gamma, n)$  spectra. If this state were  $E_2$ , a peak approximately 30 mb high, corresponding to 6 standard deviations, would have been observed in the  $(\gamma, n)$  spectrum. For an  $E_0$  assignment this fact is easily understood: The longitudinal monopole can not be excited by the pure transverse real photons.

The dipole resonance at  $81A^{-1/3}$  MeV was measured with monochromatic  $\gamma$  rays<sup>15</sup> and has also been seen in  $(e, e')$  experiments.<sup>8,9,16</sup> Remarkable agreement has been found between the two methods.

This experiment shows reasonable agreement in the angular distribution between experiment and DWBA calculations for the two forward angles, but exhibits deviations for the backward angles, an effect already found in  $N = 82$  nuclei.<sup>13</sup> We tried to explore the nature of the dipole oscillations by assuming volume and surface oscillations separately in the DWBA calculations. The results in terms of sum-rule exhaustion favor a volume oscillation (Table I). Then, however, our results are 30% smaller than the  $(\gamma, n)$  experiments.

There may be two reasons for this: (1) The  $(\gamma, n)$  measurements must be corrected for the contributions of the isovector  $E_2$  resonance to the integrated cross section. (2) Inelastic electron scattering at forward angles measures only the longitudinal matrix element  $B(C\lambda)$ . The continuity equation yields  $B(C\lambda) \approx B(E\lambda)$ , where  $B(E\lambda)$  is the transverse electric matrix element, which is the main part of the quantity measured in  $\gamma$  absorption. There is, however, another possible contribution to the total transverse matrix element, namely, the electric spin-flip contribution.<sup>9,13</sup> Following Ref. 13 we found a 20–30% contribution to the total  $B(E1)$  value possible, which would solve both problems: the difference in sum-rule exhaustion between  $(e, e')$  and  $(\gamma, n)$  and the increase of the cross section at backward angles in  $(e, e')$ .

For the resonances at 18 MeV we extracted an  $E3$  matrix element.<sup>8</sup> Backward-angle measurements in Au suggest an additional  $M2$  contribution.

No resonance has been reported up to now at 33 MeV. The angular distribution in Au exhibits  $E0$  (or  $E2$ ) character. Thus this resonance might be the isovector monopole state, proposed by Ref. 10. However, the great width in Au together with the fact that it is located at the end of our measured excitation range makes an accurate assignment very difficult.

We thank H. McFarland and D. Snyder for their hard work in keeping the Linac running.

\*Research supported by the Naval Postgraduate School Foundation Research Program.

†Work supported by a fellowship of the Deutscher Akademischer Austauschdienst.

<sup>1</sup>M. Goldhaber and E. Teller, Phys. Rev. 74, 1046 (1948).

<sup>2</sup>H. Überall, *Electron Scattering from Complex Nuclei* (Academic, New York, 1971).

<sup>3</sup>R. Pitthan and Th. Walcher, Phys. Lett. 36B, 563 (1971), and Z. Naturforsch. 27a, 1683 (1972).

<sup>4</sup>H. Tyrén and Th. A. J. Maris, Nucl. Phys. 4, 637 (1957), and 6, 446 (1958) and 7, 24 (1958).

<sup>5</sup>M. B. Lewis, Phys. Rev. Lett. 29, 1257 (1972); M. B. Lewis and F. E. Bertrand, Nucl. Phys. A196, 337 (1972).

<sup>6</sup>G. R. Satchler, Nucl. Phys. A195, 1 (1972).

<sup>7</sup>S. Fukada and Y. Torizuka, Phys. Rev. Lett. 29, 1109 (1972).

<sup>8</sup>M. Nagao and Y. Torizuka, Phys. Rev. Lett. 30, 1068 (1973).

<sup>9</sup>F. R. Buskirk, H. D. Gräf, R. Pitthan, H. Theissen, O. Titze, and Th. Walcher, Phys. Lett. 42B, 194 (1972),

and in *Proceedings of the International Conference on Photonuclear Reactions and Applications, Pacific Grove, California, 1973*, edited by B. L. Berman, CONF-730301 (Lawrence Livermore Laboratory, Livermore, Calif., 1973).

<sup>10</sup>A. Bohr and B. R. Mottelson, *Nuclear Structure* (Benjamin, New York, 1972), Vol. 2; T. Suzuki, Nucl. Phys. A217, 182 (1973).

<sup>11</sup>A. Moalem, W. Benenson, and G. M. Crawley, Phys. Rev. Lett. 31, 482 (1973); K. A. Snover, K. Ebisawa, D. R. Brown, and P. Paul, Phys. Rev. Lett. 32, 317 (1974); L. L. Rutledge, Jr., and F. C. Hiebert, Phys. Rev. Lett. 32, 551 (1974).

<sup>12</sup>R. W. Berard, F. R. Buskirk, E. B. Dally, J. N. Dyer, X. K. Maruyama, R. L. Topping, and T. J. Traverso, Phys. Lett. 47B, 355 (1973).

<sup>13</sup>R. Pitthan, Dissertation, Darmstadt University, 1972 (unpublished), and Z. Phys. 260, 283 (1973).

<sup>14</sup>M. Danos and W. Greiner, Phys. Rev. 134, B284 (1964).

<sup>15</sup>A. Veysièvre, H. Beil, R. Bergère, P. Carlos, and A. Lepretre, Nucl. Phys. A159, 561 (1970).

<sup>16</sup>Y. Torizuka *et al.*, private communication.

<sup>17</sup>X. K. Maruyama, F. R. Buskirk, E. B. Dally, J. N. Dyer, and R. Pitthan, to be published.

<sup>18</sup>S. T. Tuan, L. E. Wright, and D. S. Onley, Nucl. Instrum. Methods 60, 70 (1968).

<sup>19</sup>N. I. Kassis, Technical Report, Institut für Kernphysik der Universität Mainz, 1969 (unpublished).

<sup>20</sup>R. A. Ferrell, Phys. Rev. 107, 1631 (1957); J. Weneser and E. K. Warburton, in *The Role of Isospin in Electromagnetic Transitions*, edited by D. H. Wilkinson (North-Holland, Amsterdam, 1969).

<sup>21</sup>S. J. Skorka, J. Hertel, and T. W. Retz-Schmidt, Nucl. Data A 2, 347 (1966).

## The Widths of the E2 ( $\Delta T = 0$ and $\Delta T = 1$ ) Giant Resonances in $^{165}\text{Ho}^*$

G. L. Moore, F. R. Buskirk, E. B. Dally, J. N. Dyer,  
X. K. Maruyama <sup>†</sup>, and R. Pitthan

Department of Physics and Chemistry, Naval Postgraduate School, Monterey, CA 93940, USA

(Z. Naturforsch. 31 a, 668–669 [1976];  
received March 20, 1976)

Inelastic electron scattering confirms broadening of the isoscalar ( $\Delta T=0$ ) E2 giant resonance in  $^{165}\text{Ho}$  as compared to spherical nuclei. Discrepancies in magnitude between results of other experiments are reconciled. The isovector ( $\Delta T=1$ ) E2 giant resonance is, for the first time, observed to be split into at least two parts.

Since the discovery of giant resonances with a multipolarity different from E1 much information using various excitation methods has been collected concerning the E2 ( $\Delta T=0$ ) resonance at  $E_x = 63 \text{ A}^{-1/3} \text{ MeV}^1$ . Less information has been reported concerning the other resonance identified, the M1 giant resonance, and even less is known for the E2 ( $\Delta T=1$ ) isovector giant resonance around  $130 \text{ A}^{-1/3} \text{ MeV}$ , which was mentioned, but not identified with certainty in the same paper. The information available concerning the latter has been collected recently by Paul <sup>2</sup>.

Although the best data available are from electron scattering, their accuracy has been hampered by the uncertainty in the calculation of the radiation tail. This uncertainty may be overcome in the investigation of isolated low-lying levels by interpolating a fitted smooth background between regions in the spectrum without lines. In the region of the giant dipole resonance the radiation tail is determined by fixing the background through the known strength and natural width of the E1 resonance. No such remedy is possible in the higher continuum above the giant dipole resonance and better radiation tail calculations are needed. Heuristic insertion of all known practical improvements in the theoretical calculation of the radiative tail into a fitting routine has led to the result that the calculated radiation tail now accounts for virtually all radiative background in our measurements, a fact which opens up new possibilities for the investigation of the higher energy resonances.

The experiment reported here was carried out with electrons of a primary energy between 60 and 105 MeV from the 120 MeV linear electron

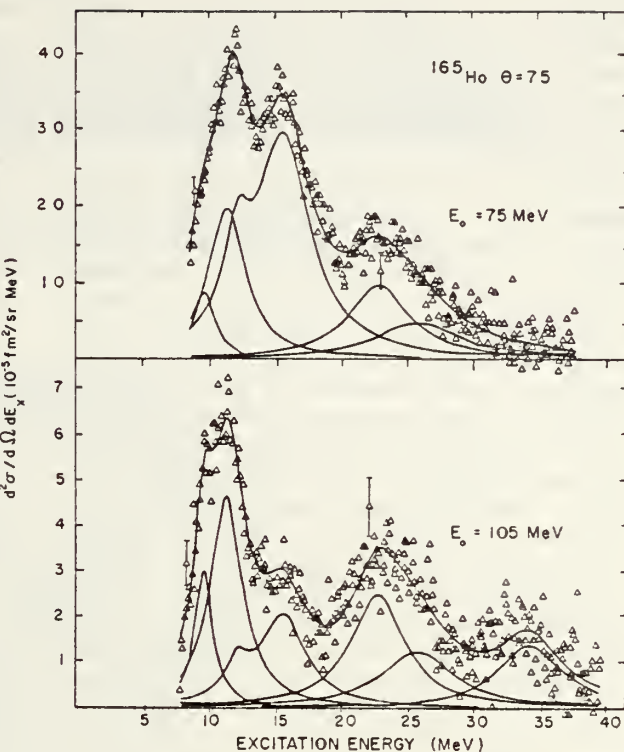


Fig. 1. Spectrum of 75 and 105 MeV electrons, scattered inelastically from  $^{165}\text{Ho}$  at a scattering angle of  $75^\circ$ . The resolution is 500 keV. The background which consists of the radiation tail and the machine background has been subtracted. Note that the relative strength of the E1 and E2 resonances more than reverses, if one goes from 75 MeV to 105 MeV. Typical raw spectra; i.e., background not subtracted, may be found in Ref. <sup>4</sup>. The form of the E1 resonance was taken from  $(\gamma, n)$  measurements (Ref. <sup>9</sup>); the height was fitted. The energy weighed sum rule exhaustion found for the E1 resonance is 108%, in excellent agreement with the values reported in Ref. <sup>9</sup>, thus proving the reliability of the background subtraction.

accelerator of the Naval Postgraduate School, a three-section LINAC of the Stanford type <sup>3</sup>. This investigation was specifically undertaken to show whether or not the giant quadrupole resonances are split or broadened in a deformed nucleus. Earlier experiments in  $^{208}\text{Pb}$  and  $^{197}\text{Au}$  had shown a gradual broadening of all the electric resonances observed as one proceeds from the spherical doubly magic nucleus  $^{208}\text{Pb}$  to the non-magic  $^{197}\text{Au}$ . The latter still has a (quasi) spherical ground state, so that the observed broadening of the giant resonances, as compared to  $^{208}\text{Pb}$ , can only be explained as due to dynamic deformation <sup>4</sup>.  $^{165}\text{Ho}$  was chosen as the target nucleus because it is highly deformed and it lies between  $^{140}\text{Ce}$  and  $^{208}\text{Pb}$ , in which we had evaluated the giant quadrupole ( $\Delta T = 0$ ) resonance using similar techniques. The mea-

\* Supported in part by the National Science Foundation and the Naval Postgraduate School Research Foundation.

<sup>†</sup> Now at National Bureau of Standards, Washington D.C., 20234, USA.

surements were restricted to a forward scattering angle of  $75^\circ$ , in order to avoid complications with transverse contributions<sup>1, 4</sup>. A more detailed account of our experiment will be published elsewhere; here we will report our findings for the E2 resonances.

The single most important result is the observed splitting of the isovector giant resonance into two parts at 23 and 26 MeV excitation energy (Figure 1). The strength ratio of the two components is observed to be 3:2. They both follow separately an E2 DWBA calculation<sup>5</sup> and together they comprise  $(100 \pm 30)\%$  of the E2 sum rule. No other experiments on the isovector E2 giant resonances in deformed nuclei have been reported.

This result agrees with what one would expect from the extrapolation of the results in  $^{208}\text{Pb}$  and  $^{197}\text{Au}$ , as implied by the observed splitting of the E1 resonances due to the (dynamic) deformation of the nuclei in the continuum. It is also in qualitative agreement with the results of a perturbation theory calculation where the effect of the deformed ground state is represented by adding to the spherical potential a term proportional to  $Y_{20}$ , in analogy to calculations for the E1 ( $\Delta T=1$ ) resonance.

The result for the low lying E2 ( $\Delta T=0$ ) resonance is displayed in Table I and compared with the best available values. The broadening observed in this experiment,  $\Gamma_{\text{deformed}} - \Gamma_{\text{spherical}}$ , agrees with the corresponding result in the  $(\alpha, \alpha')$  experi-

ment<sup>6</sup>, but the absolute widths are smaller. However, it has already been observed that the widths of resonances excited by slow hadronic interacting particles generally are greater than that found from the electromagnetic processes<sup>7</sup>. The disagreement with the results from Nd arises from the fact that the effects of the resonance at 9.8 MeV ( $53 \text{ A}^{-1/3}$  MeV) were taken into account in the present experiment. From the  $^{165}\text{Ho}$  data alone one would not be able to conclude definitively the existence of this resonance. But a resonance at the corresponding energy of  $53 \text{ A}^{-1/3}$  MeV has consistently been seen in many nuclei between  $^{58}\text{Ni}$ <sup>8</sup> and  $^{208}\text{Pb}$ <sup>4</sup>. All the different electric excitation modes discovered so far have exhibited a very smooth dependence of strength and excitation energy as a function of A, so that the assumption of its presence seems well justified. If we do not assume the presence of this resonance we find  $\Gamma_{\text{nat}} = (5.1 \pm 0.3)$  MeV, in agreement with<sup>7</sup>. In turn, we conclude that with this resonance taken into account, the value for  $^{150}\text{Nd}$  would be in agreement with ours for  $^{165}\text{Ho}$ , which would bring all the measured relative broadenings in Table I in agreement.

Since the deformation of the three deformed nuclei is practically identical<sup>9</sup>, one would expect a similar broadening, an expectation which is supported by the fact that the E2 ( $\Delta T=0$ ) resonances in spherical nuclei as different as  $^{140}\text{Ce}$  and  $^{208}\text{Pb}$  have the same width.

Table I. Comparison of the natural width of E2 ( $\Delta T=0$ ) resonances in spherical and deformed nuclei. The fifth column shows that the splitting of the giant dipole resonance, i. e., the deformation of the nucleus at about 14 MeV excitation energy, is practically identical in the deformed nuclei considered.

Excitation Method	$\Gamma_{\text{spherical}}$ [MeV]	$\Gamma_{\text{deformed}}$ [MeV]	$\Delta\Gamma$ [MeV]	$\Delta E_1$ [MeV] <sup>a</sup>	$E_x \cdot B(E2)$ [%]
(e, e')	$2.8 \pm 0.2$ ( $^{142}\text{Nd}$ ) <sup>b</sup>	$5.0 \pm 0.2$ ( $^{150}\text{Nd}$ ) <sup>b</sup>	2.2	3.74	88
( $\alpha, \alpha'$ )	$3.9 \pm 0.2$ ( $^{144}\text{Sm}$ ) <sup>c</sup>	$4.7 \pm 0.3$ ( $^{154}\text{Sm}$ ) <sup>c</sup>	0.8	3.57	102
(e, e')	$2.8 \pm 0.2$ ( $^{140}\text{Ce}$ ) <sup>d</sup>	$4.0 \pm 0.4$ ( $^{165}\text{Ho}$ ) <sup>e</sup>	1.2	3.53	75
	$2.8 \pm 0.3$ ( $^{208}\text{Pb}$ )				

<sup>a</sup> Ref. <sup>9</sup>; <sup>b</sup> Ref. <sup>7</sup>; <sup>c</sup> Ref. <sup>6</sup>; <sup>d</sup> Ref. <sup>1, 4</sup>; <sup>e</sup> this work.

<sup>1</sup> R. Pitthan and Th. Walcher, Z. Naturforsch. **27a**, 1683 [1972].

<sup>2</sup> P. Paul, Internat. Symposium on Highly Excited States in Nuclei, Jülich, September 1975, Proceedings, Vol. 2.

<sup>3</sup> R. W. Berard, F. R. Buskirk, E. B. Dally, J. N. Dyer, X. K. Maruyama, R. L. Topping, and T. J. Traverso, Phys. Lett. **47 B**, 355 [1973].

<sup>4</sup> R. Pitthan, F. R. Buskirk, E. B. Dally, J. N. Dyer, and X. K. Maruyama, Phys. Rev. Lett. **33**, 849 [1974]; Phys. Rev. Lett. **34**, 848 [1975].

<sup>5</sup> S. T. Tuan, L. E. Wright, and D. S. Onley, Nucl. Instrum. Methods **60**, 70 [1968].

<sup>6</sup> T. Kishimoto, J. M. Moss, D. H. Youngblood, J. D. Bronson, C. M. Rosza, D. R. Brown, and A. D. Bacher, Phys. Rev. Lett. **35**, 552 [1975].

<sup>7</sup> A. Schwierczinski, R. Frey, E. Spamer, H. Theissen, and Th. Walcher, Phys. Lett. **55 B**, 171 [1975].

<sup>8</sup> I. S. Gulkarov, N. G. Afanasev, V. M. Khvastunov, N. G. Shevchenko, V. D. Afanasev, G. A. Savitskii, and A. A. Khomich, Sov. J. Nucl. Phys. **9**, 272 [1969].

<sup>9</sup> B. L. Berman and S. C. Fultz, Rev. Mod. Phys. **47**, 713 [1975].

# NAVAL POSTGRADUATE SCHOOL

## Monterey, California



The Natural Line Shape of the Giant Dipole Resonance<sup>+</sup>

E.F. Gordon and R. Pitthan  
Department of Physics and Chemistry

<sup>+</sup>Supported by the National Science Foundation and the Naval Postgraduate School Research Foundation

## I. INTRODUCTION

In the attempt to fit inelastic electron scattering data in the Giant Resonance region with assumed resonance line shapes and a background based, but not totally determined, on the theoretically calculated radiation tail one finds a significant interdependence between the assumed line shapes and background subtractions. In addition, the mutual effects that neighboring resonances have on each other certainly depends on their assumed line shapes. It therefore seems evident that the choice of line shape is crucial to the proper assignment of resonance energies and their relative strengths.

Three line forms to be considered are the Gaussian, Breit-Wigner and Lorentz shapes. In the following  $(d^2\sigma/d\Omega dE_x)$  = differential cross section  
 $E_x$  = excitation energy  
 $\Gamma$  = the full width at half maximum (FWHM)  
 $E_0$  = excitation energy of the maximum.

The Breit-Wigner form  

$$\frac{d^2\sigma(E_x)}{d\Omega dE_x} = \left( \frac{d^2\sigma}{dE_x^2} \right)_{\text{max}} \frac{E_x^2 \Gamma^2}{(E_x - E_0)^2 + E_x^2 \Gamma^2}$$
 is symmetric about  $E_0$ .

Area (Breit-Wigner) =  $\pi(\Gamma/2) (d^2\sigma/d\Omega dE_x)_{\text{max}}$ .  
 The Lorentz form  

$$\frac{d^2\sigma(E_x)}{d\Omega dE_x} = \left( \frac{d^2\sigma}{dE_x^2} \right)_{\text{max}} \frac{(\Gamma/2)^2}{(E_x - E_0)^2 + (\Gamma/2)^2}$$

I-2  
 I-1  
 I-3  
 describes an asymmetric variation of the differential cross section about the peak energy.

ABSTRACT

Investigation of photoabsorption experiments in the spherical nucleus  $^{141}\text{Pr}$ , the quasispherical dynamically deformed  $^{197}\text{Au}$ , and the statically deformed  $^{165}\text{Ho}$  showed that the function which describes best the energy dependence of the reduced transition probability is given by the Breit-Wigner form rather than the Lorentz form. However, the form of the resulting measured cross section is approximately of the Lorentz type. The dependence of the giant resonance width  $\Gamma$  on the excitation energy was also investigated, and found to be less than 1% per MeV if one considered the known isovector E2 resonance above the giant dipole resonance. Best fit values of the reduced transition probabilities for the three nuclei are given and compared to  $(e,e')$  results.

$$\text{Area (Lorentz)} = \pi(\Gamma/2) (\frac{d^2\sigma}{d\Omega dE_x})_{\max} \quad I-4$$

Note that the limits of integration are  $-\infty$  to  $+\infty$  for Breit-Wigner, and 0 to  $+\infty$  for the Lorentz form (see II.A). The Gaussian form

$$\frac{d^2\sigma(E_x)}{d\Omega dE_x} = \left( \frac{\frac{d^2\sigma}{dE_x}}{d\Omega dE_x}_{\max} \right)^2 \exp \left[ -\left( \frac{E_x - E_0}{\Gamma/2} \right)^2 \right] \quad I-5$$

is symmetric about the peak energy.

$$\text{Area (Gauss)} = (\Gamma/2) \sqrt{\pi/\ln 2} (d^2\sigma/d\Omega dE_x)_{\max} \quad I-6$$

These three line forms are plotted in Figure 1 for  $^{197}\text{Au}$ .

Different investigators have assumed different line shapes in their attempts to fit their cross section data. The Gaussian line shape, which could not be justified by purely physical argument, was used mainly because of its mathematical simplicity. The E1 resonance in photonuclear experiments has been fitted with both the Breit-Wigner and Lorentz forms. Because the E1 cross section has been measured to be asymmetric, the Lorentz form has been preferred more recently because it yields a better fit far off resonance (several fm's) at the higher excitation energies [1].

The primary goal of electron scattering experiments is the determination of the intrinsic reduced transition probability (B-value) per unit energy interval,  $dB/dE_x$ , via the measured scattering cross section. It is the first quantity, which, when integrated over energy, yields the total reduced transition probability  $B(E)$ . One is left with the problem of determining the relationship between  $d^2\sigma/d\Omega dE_x$  and  $dB/dE_x$ .

If one defines an "excitation factor"  $f(E_x)$  by

$$\frac{d^2\sigma}{d\Omega dE_x} = C_1 f(E_x) \frac{dB}{dE_x}, \quad I-7$$

$d^2\sigma/d\Omega dE_x$  will yield the distribution of the desired reduced transition probability. Equation I-7 can be rewritten as (response function) = (excitation factor)  $\times$  (excitation strength function). The left side of the equation corresponds to the data to be fitted; the right side corresponds to the fitting line shapes as modified by the excitation factor. Note that in the following sections the excitation factor is defined in such a way that the numerical value is identical to 1.0 at  $E_0$  and corresponds to a constant B-value distribution of  $B(E) = 1 \text{ fm}^{2\lambda}$ . Note furthermore, that  $E_0$  is, therefore, not the energy associated with the maximum cross section, but is that energy corresponding to the maximum of the excitation strength function (B-value).

By a comparison of the results obtained from applying each of the three line shapes, including the effect of the given choice of line shape is preferred over the others, that is, that the line shape question may be solved experimentally, at least for ( $\gamma, \text{abs}$ ). Since this work considers only heavy nuclei, in which the Coulomb barrier is high, the approximation  $\sigma(Y, \text{abs}) = J(Y, n) + \sigma(Y, 2n) + \sigma(Y, np)$  is used.

Closely connected with the question of the resonance line shape is the problem of the resonance width. Presently

no successful quantitative microscopic theory of giant resonance widths exists.

A macroscopic approach using the concept of viscosity and the hydrodynamic model shows an overall agreement with the width of giant resonances as a function of the nuclear mass, but does not address the problem of the width as a function of excitation energy within one given resonance in a certain nucleus [2].

### III. THEORETICAL AND EXPERIMENTAL BACKGROUND

#### A. Line Shapes

Since the experimental line shape of the GDR is asymmetric, mostly the Lorentz form has been preferred [see, e.g. Ref. 3]. Danos and Greiner [4] investigated this problem theoretically. Regarding the E1 absorption of a photon as an entrance channel (doorway state) whose energy is distributed through a succession of residual interactions among actual compound states in the energy interval around  $E_0$ , one is led to the same results as for a resonant scattering event described by a Breit-Wigner form. Unfortunately the authors do not make a clear distinction between strength functions (reduced transition probabilities) and photon cross sections.

In later papers [5] the same authors showed that one is led to a Lorentz term using the argument that since the photon has no rest mass and using the concept of time reversal, one must choose a function which has symmetric energy poles with respect to the imaginary axis. This description technique allows one to consider the photon absorption cross section as a superposition of a number of individual Lorentz lines [3]. Again there seems to be confusion between the derived matrix elements and experimentally measured cross sections. Most authors have generally adopted the practice of representing the form of the measured photonuclear absorption cross section of the giant resonance for heavy spherical nuclei by a single Lorentz line and for heavy deformed nuclei by two Lorentz lines [1].

Since the radiation background in inelastic electron scattering experiments is very high, it is unlikely that the choice between the Breit-Wigner and Lorentz forms, which are very similar (Equations I-1, 3), can be easily made for ( $e$ ,  $e'$ ). Fortunately photo-nuclear reaction data taken with monochromatic photons [1] do not have this background problem and are, therefore, more suited experimentally for studying the problem of a line shape choice, at least for the E1 state. This paper concentrates, therefore, on photon experiments. Note that the photo-absorption experiments discussed here measure  $d\sigma/dE_x$  only, and not  $d^2\sigma/d\Omega dE_x$ .

The connection between the reduced transition strength and the photoabsorption cross section is given by [6]

$$\int_{E_1}^{E_2} \sigma_Y dE_Y = \pi^2 \hbar c a \frac{8\pi(\lambda+1)\lambda^{-1}}{(2\lambda+1)!!} \frac{1}{2} k^{2\lambda-1} B(\lambda, k) , \quad \text{II-1}$$

where  $\sigma \equiv d\sigma/dE_x$ . It follows that

$$d\sigma/dE_x = C_2 (E_x/E_O) (dB(E1, k)/dE_x) , \quad \text{II-2}$$

when  $\lambda = 1$ . Therefore, for photoexcitation of a dipole resonance the excitation factor is given by  $E_x/E_O$ . This can be re-expressed as

$$f(E_x) = 1 + (E_x - E_O)/E_O , \quad \text{II-3}$$

Note that  $f(E_x)$  is normalized to unity at the resonance maximum and that it is linear in the excitation energy.

The Lorentz form can be mathematically decomposed into a superposition of two Breit-Wigner forms as follows:

$$\left( \frac{d\sigma}{dE_x} \right)_{\text{Lor}} = \left( \frac{d\sigma}{dE_x} \right)_{\text{max}} \frac{\frac{E_x}{E_{\text{res}}}}{\left[ \frac{(\Gamma/2)^2}{(E_x - E_{\text{res}})^2 + (\Gamma/2)^2} \right]} - \left[ \frac{\frac{(\Gamma/2)^2}{(E_x + E_{\text{res}})^2 + (\Gamma/2)^2}}{\left[ \frac{(\Gamma/2)^2}{(E_x - E_{\text{res}})^2 + (\Gamma/2)^2} \right]} \right] , \quad \text{II-4}$$

where  $E_{\text{res}}^2 = E_O^2 - (\Gamma/2)^2 \ll E_O^2$ , the latter approximation being good for giant resonances. In the analysis of individual resonances one usually omits the negative energy resonance term since it contributes a practically constant cross section of less than 1% for  $E_x \neq E_{\text{res}}$  and since away from resonance there may be more important additional contributions arising from other neighboring and distant resonances [7].

Applying the last three equations to the photoexcitation of a giant dipole resonance and assuming an intrinsic Breit-Wigner line shape for  $dB/dE_x$ , one can see that the resulting measured cross section has a Lorentz shape, given by

$$(d\sigma/dE_x)_{\text{Lor}} \approx C_2 (E_x/E_O) (dB/dE_x)_{\text{BW}} , \quad \text{II-5}$$

where one has neglected the negative branch of the Lorentz curve for the reasons previously cited. If one compares the two sides of Equation II-5 for heavy nuclei, e.g.,  $^{197}\text{Au}$ , one observes indeed that this approximation is very good with a

nearly constant small difference. It will be shown later that due to the high accuracy of modern photo absorption experiments even differences of this order have a great impact on the line shape experimentally found. The integrated cross section which results

$$\int_{-\infty}^{\infty} \frac{dE_x}{E_0} \left( \frac{d\sigma}{dE_x} \right)_{BW} dE_x \approx \int_0^{\infty} \left( \frac{d\sigma}{dE_x} \right)_{Lor} dE_x = \frac{\pi r}{2} \left( \frac{d\sigma}{dE_x} \right)_{max} \quad II-6$$

can be seen to be only slightly dependent on the assumed line shape. Note, though, that the limits of integration are not identical, but this convention is widely used [3].

In summation it may be argued that  $f(E_x)$  as defined above for the photoexcitation of a giant dipole resonance is identical with the term which, in a very good approximation, makes up for the difference between the Breit-Wigner and Lorentz forms. This is only true for an E1 resonance, since Equation II-1 shows that for the photoexcitation of an E2 resonance

$$f(E_x) = C_3 (E_x/E_0)^3 \quad II-7$$

Alternatively it may be stated that the excitation factor  $f(E_x)$  produces the apparent asymmetry in the cross section due to the rapidly changing momentum transfer

$$k = E_x/\hbar c \quad II-8$$

In inelastic electron scattering the momentum transfer is described by

$$q^2 = (4E_f E_i / \hbar^2 c^2) \sin^2(\theta/2), \quad II-9$$

where  $E_x = E_i - E_f$ . It is seen that the momentum transfer for  $(e, e')$  does not change as rapidly with excitation energy as for  $(\gamma, abs)$ . Even if the momentum transfer does not change as rapidly in  $(e, e')$  as for  $(\gamma, abs)$ , the resulting effect on  $f(E_x)$  is not negligible. This is shown in Figure 2, which compares the energy dependence of  $f(E_x)$  for  $(e, e')$  and  $(\gamma, abs)$  in the region of the giant dipole resonance in  $^{197}\text{Au}$  in the case of 65 MeV electrons.

Heretofore the excitation factor has been given as one possible reason for the measured cross section being asymmetric. In electron scattering, the incremental sampling of the resonance curve by the line shape of an elastic peak, which is used to reflect the line shape of the sampling line, will introduce other asymmetry. The sampler's effect may in principle be considered as a superposition of two phenomena, asymmetry and the radiative tail. The asymmetric part gives rise to a shift toward higher energy of the whole curve with a right half width at half maximum (HWHM) being slightly larger than its left counterpart. However, this difference typically has been

found to be only 20 kev for a full width of 200 kev for the elastic line. An asymmetry of 20 kev for a line width of several Mev as in the case of the giant resonances will give rise to a

negligible shift only. The radiative tail which causes at least part of the asymmetry in the elastic line shape (sampler) would give rise to detrimental effects only for energies far off resonance; however, the cross section has already dropped to values no larger than three percent of the peak height at an excitation energy of only two sampler half widths away from the maximum. This effect is small compared to the uncertainty arising from the underlying radiative tail. For these reasons the fitting programs used in the evaluation of these line shapes have assumed equal and constant right and left HWHM's for the mathematical expressions for the Giant Resonances.

Another effect which would lead to asymmetric line shapes is the fact that the width might be a function of excitation energy. This possibility has to be investigated, too.

#### B. Energy Dependence of Giant Resonance Width

Evidently any mathematical expression used in fitting the experimental total photoabsorption cross section curve requires a spreading parameter which characterizes the fact that the giant dipole resonance has the experimental width  $\Gamma$  as one of its interesting parameters. Various attempts to explain this width can be found in Ref. [5,8,9,10,11,12] and especially Ref. [2]. The only analytical form used in the literature is that first given by Danos and Greiner [4] who assumed a power law dependence

$$\Gamma = C E_0^{-\delta}, \quad \text{III-10}$$

with  $C$  and  $\delta$  to be determined from the fitting to the data. They found  $\delta$  to be 2.2 for  $^{165}\text{Ho}$ . Ambler et al. [13] found  $\delta$  to be 2.0 for  $^{165}\text{Ho}$ .

Carlos et al. [11] proposed a semi-phenomenological description of the giant dipole resonance. They tried to attribute the width to three sources: (1) the decay width  $\Gamma^+$  (typically 100 kev), (2) a spreading width  $\Delta\Gamma$  due to coupling between dipole oscillations and surface quadrupole motion and (3) a damping width  $\Gamma^+$ . Having thus defined

$$\Gamma = \Gamma^+ + \Delta\Gamma + \Gamma^+, \quad \text{III-11}$$

and having chosen a set of nuclei for which  $\Gamma^+$  and  $\Delta\Gamma$  are believed to be small, they studied  $\Gamma^+$  directly for medium and heavy nuclei. They obtained as an empirical law for the damping width

$$\Gamma^+ = (0.026 \pm 0.0005) E_*^{(1.9 \pm 0.1)}, \quad \text{III-12}$$

for  $139 \leq A \leq 238$ ,

where all energies are in MeV, as in the previous equations. Commenting on the results of Carlos et al., Berman and Fultz [1] stated that the use of a simple power law dependence of  $\Gamma$  on  $E$  is fruitless or is of use only in a limited mass region; and that unless one takes into account shell effects, or the resultant level density in the giant resonance region, one cannot generalize the behavior of the giant resonance width in this way.

All the previously cited references on experimental findings have attempted to find the energy dependence of the giant resonance widths by correlating their experimentally determined constant widths to their experimentally determined resonance energies. Their data base has extended either over several different excitation modes of a given nucleus or over the same mode of excitation for several nuclei. In other words they have attempted to find the widths as a function of the resonance energy.

It is a second goal of this paper to determine if, for a given excitation mode of a given nucleus, the width of the giant resonance varies continuously with the excitation energy. Generalizing the concept of Danos and Greiner [4], one can use the expression

$$\Gamma = \Gamma_o (E_x/E_o)^\delta, \quad \text{II-13}$$

as shown in Figure 3 for  $^{197}\text{Au}$ , where  $\delta = 2.0$  and  $\Gamma_o$  equals the experimentally determined FWHM. One easily sees from this figure that the dependence of  $\Gamma$  on the square of the excitation energy yields unreasonable high cross sections. This work therefore uses the heuristic linear expression

$$\Gamma(E_x) = \Gamma_o [1 + \epsilon(E_x - E_o)] \quad \text{II-14}$$

to investigate a linear dependence of the width on the excitation energy. This expression may be regarded as a Taylor series of  $\Gamma$  in  $E_x$  which neglects second and higher order terms.

### III. FITTING PROCEDURES AND RESULTS

Nuclei with varying degrees of deformation, which have been measured with both monochromatic photon and inelastic electron scattering experiments, were sought for this investigation. The spherical nucleus  $^{141}\text{Pr}$  [14, 15], the statically deformed  $^{165}\text{Ho}$  [16, 17], and the dynamically deformed  $^{197}\text{Au}$  [3, 18] fulfilled these requirements.

Both the photonuclear and electron scattering data were fit with a least-squares fitting procedure. To meet the objectives of this paper all three line shapes, Gauss, Breit-Wigner and Lorentz, were incorporated into the fitting program. This program afforded the investigator many options in fitting giant resonance curves. Any portion of the furnished data could be fit with a variable number of lines with any combination of line shapes of fixed or variable resonance energy, width and peak height. A best fit is determined when a minimum in chi-square  $\chi^2$  was found. Chi-square is defined as

$$\chi^2 = \sum_i (x_i - x_o)^2 / \sigma_i^2 \quad \text{III-1}$$

where  $x_i$  = calculated value of the cross section  
 $x_o$  = measured value of the cross section  
 $\sigma_i$  = experimental error associated with  $x_i$ .

Related to this chi-square distribution is the term "degrees of freedom" which is defined as the number of points to be fitted minus the number of fitting parameters. The minimization

of  $\chi^2$  (per degree of freedom) offers the following advantages:

If the value of  $\chi^2$  is appreciably greater than unity, the fitted line shape is incorrect, while if the value of  $\chi^2$  is appreciably less than unity, the experimental statistics are incorrect. Using this criterion, one can make a choice between different line shapes or between a one line or a two line fit for cases such as  $^{197}\text{Au}$ . Additionally, since the  $^{197}\text{Au}$  fits often gave a  $\chi^2$  per degree of freedom of less than 0.25, it was assumed that the errors in the data given by the authors were too large by a factor of two. Therefore, the resulting  $\chi^2$  per degree of freedom was arbitrarily multiplied by four for all  $^{197}\text{Au}$  fits. Naturally this had no effect on the fits themselves, but makes the direct comparison between the three nuclei easier. The variance of  $\chi^2$  was approximately 0.15 for all three nuclei.

The photonuclear data were fit with each of the three line shapes. Since the Gaussian form resulted in an unacceptably large  $\chi^2$  for any of the fits, this form was discarded. These initial fits were followed by ones in which the excitation factor  $f(E_x)$  was taken into account (Figures 4-7). A further test of the concept of the excitation factor was made using

$$f(E_x) = 1 + \frac{1}{E_0} + \alpha(E_x - E_0) . \quad \text{III-2}$$

By varying  $\alpha$  in steps it was to be determined whether  $f(E_x)$  in the form of Equation III-3 accounted for the total variation of  $d\sigma/dE_x$  as a function of the excitation energy  $E_x$ . If so,  $\alpha$  should be close to zero (Figure 8).

The final objective of determining the functional dependence of the giant resonance width on the excitation energy was to be met by obtaining best fits for different values of  $\epsilon$  (Equation II-14) and comparing the resulting  $\chi^2$ .

Table I shows most of the quantitative results of this investigation. Those energies and widths that were held fixed show no errors.

Compared to the results of Ref. 1, larger fitting intervals were possible in this investigation. While the extracted areas are close to those of Ref. 1, they are consistently smaller, as are the widths. This effect is due in part to the subtraction of the cross section due to the isovector ( $\Delta T = 1$ ) E2 state(s). Note again that this paper aims at the more fundamental quantity of the reduced transition probability rather than at the excitation cross section, which varies with experimental method, and that, therefore, the parameters extracted are the parameters of the excitation strength function and not of the cross section. The excitation factor was neglected for the E2 resonances. Without exception the best  $\chi^2$  was obtained for the Breit-Wigner line shape multiplied by the excitation factor. Both the Breit-Wigner and Lorentz line shapes gave better values of  $\chi^2$  with  $f(E_x)$  than without  $f(E_x)$ .

Table II shows the percentages of the Thomas-Reiche-Kuhn (TRK) sum rule [19] exhausted by the best Breit-Wigner fits of the E1 lines. This sum rule gives the total integrated cross section for electric dipole photon absorption and is defined

$$\int_0^\infty \sigma(E) dE = 60(NZ/A) \text{ MeV-mb} . \quad \text{III-3}$$

Also given are the B-values for both the photonuclear and inelastic electron scattering experiments. The Goldhaber-Teller model (surface oscillations) was used to extract the B-values from the  $(e, e')$  experiments [15,17,18]. Both the  $^{141}\text{Pr}$  and  $^{165}\text{Ho}$  values agree very well, but there is a significant difference between the two values for  $^{197}\text{Au}$  (for a possible explanation see Ref. 18).

The shapes of the  $\alpha$ -curves (Figure 8) varied with the three elements. The deformed nuclei have wide minima for  $\alpha = 0.04$  for the Breit-Wigner curves with the  $^{165}\text{Ho}$  curve being steeper than the  $^{197}\text{Au}$  curve. Note that the  $\chi^2$  was re-normalized for purposes of comparison. A sharp minimum at  $\alpha = 0$  characterizes the  $^{141}\text{Pr}$  curve. Contained in Table III are the fitting parameters for  $^{141}\text{Pr}$  obtained with different values of  $\alpha$ .

One observes that as  $\alpha$  increases the parameters for the resonances change systematically. Differences in the area under the E1 curve are compensated for by the area under the E2 curve. This emphasizes once more the importance of the excitation factor for the evaluation of giant resonances, especially weak ones besides strong ones.

By comparing the one and two E1 line fits for  $^{197}\text{Au}$  (Figure 5,6), one observes that a better fit was obtained for the latter. The splitting of the giant dipole resonance

resulted in a reduction of  $\chi^2$  by a factor of five. The  $\chi^2$  was reduced even further by considering the E2( $\Delta T = 1$ ) state at 23.0 MeV [18] (Figure 5). Although this line was outside the range of the available data, the effect within the fitting range was detectable. The peak height of this line, which was allowed to vary, was 23 mb as compared to the  $(e, e')$  [18] result of 31.5 mb calculated with equation II-1. In all other  $^{197}\text{Au}$  fits the energies, widths, and peak heights were allowed to vary.

Isovector E2 lines at 23.5 and 26.75 MeV [17] were used in the  $^{165}\text{Ho}$  fits. A variation of  $\pm 0.5$  MeV for these energies had no appreciable effect on the  $\chi^2$ , but the exclusion of these lines increased the  $\chi^2$  most significantly. The results for these two lines should be considered qualitatively rather than quantitatively. All other reported parameters for  $^{165}\text{Ho}$  were allowed to vary.

Similarly an E2 line at 25.6 MeV was used in  $^{141}\text{Pr}$  [15]. The resonance width of this line was fixed at 4.0 MeV while the remainder of the fitting parameters varied. For the  $\epsilon$  distribution (Equation II-14) it was found that both  $^{197}\text{Au}$  and  $^{141}\text{Pr}$  showed a minimum  $\chi^2$  for  $\epsilon = 0$ , while  $^{165}\text{Ho}$  achieved a minimum  $\chi^2$  for  $\epsilon = -0.02$ . If one takes this result seriously, it would imply that the resonance width shrinks for increasing excitation energies which seems physically untenable. One should rather conclude that the interdependence between the not too well known structures around 25 MeV and the E1 resonances bring this effect about. In any case this

investigation shows that the change of  $\Gamma$  is smaller than 1% per Mev for the spherical and quasispherical nuclei and consistent with zero.

IV. CONCLUSIONS

Of the three line shapes considered the Gaussian form can definitely be discarded. Reasonable values of  $\chi^2$  for the Gaussian form resulted only for multiple line fits, even for the spherical nucleus  $^{141}\text{Pr}$ . Even though reasonable, these values of  $\chi^2$  were much worse than the corresponding values of  $\chi^2$  for the Lorentz and Breit-Wigner forms.

The choice between the Breit-Wigner and Lorentz line shapes is less obvious. If one compares the values of  $\chi^2$  for  $^{197}\text{Au}$  in Table I for the Lorentz form (7.21, Figure 6a) and the Lorentz approximation (1.17, Figure 6e), the latter corresponding to a Breit-Wigner form with the excitation strength factor, the choice seems trivial. However, we mentioned the nearly constant difference between the two line shapes. It represents a 0.7% deviation since the peak height is normalized to unity. The standard deviation is (4-6%). Keeping in mind that this work halved these errors, one calculates a change in the values of  $\chi^2$  of 2.8 to 6.2. This result explains most of the difference between the values of  $\chi^2$  for the Lorentz form without the excitation factor and the Breit-Wigner form with the excitation factor. Additionally this result illustrates not only the accuracy achieved by monochromatic photon experiments but also the importance of the line shape selection.

Further complicating the choice between the two forms is the interdependence between the effect of the excitation factor

$f(E_x)$  and the consideration of the E2 isovector lines. With  $f(E_x)$  multiplying the line shapes the decreased significantly for all three nuclei, regardless of line shape selection.

The results for  $^{197}\text{Au}$  show that  $^{197}\text{Au}$  is dynamically deformed at an excitation energy of 13 Mev, the deformation being about one third of that found for  $^{165}\text{Ho}$ . Moreover, if one chooses the "right" line shape (Breit-Wigner form), the ratio of the two B-values is close to 1:2 for the resonance at the lower energy compared to the resonance at the higher energy as expected for deformed nuclei [20].

Because the Breit-Wigner line shape multiplied by the excitation factor consistently gave better fits to the data and agrees better with the isovector quadrupole strength from electron scattering than the Lorentz form, the distribution of the reduced transition probability is concluded to be of Breit-Wigner form. This result is especially satisfying since the theoretical reasoning for a Breit-Wigner shape is simpler and is founded on more basic nuclear properties than is the Lorentz shape (see Ref [4,5]). The cross section is concluded to be of the Lorentz shape, insofar as the approximation of Equation III-5 holds.

Every aspect of this investigation confirmed the concept of the excitation factor. Values of  $\chi^2$  were reduced by factors of 2-7 by using this factor. Even the Lorentz shape gave better fits when multiplied by  $f(E_x)$ . The extremely sharp minimum in the  $^{141}\text{Pr}$   $\alpha$  curve (Figure 9) and the broad minima regions

near  $\alpha = 0.0$  in  $^{165}\text{Ho}$  and  $^{197}\text{Au}$  show that the form of  $f(E_x)$  in Equation II-3 is essentially correct.

It is disturbing that the absolute  $\chi^2$ -minima for  $^{165}\text{Ho}$  and  $^{197}\text{Au}$  were achieved for  $\alpha = 0.04$ . In the case of these deformed nuclei with their resonances overlapping, the fitting parameters are very interdependent, a fact which is reflected in the opening of the  $\chi^2$ -parabolas for the different nuclei of Figure 9.

There was no evidence of a dependence of the giant dipole resonance width on the excitation energy in the first order approximation used (III-15).

Figure 1

Comparison of Gauss, Breit-Wigner and Lorentz line shape for the parameters of the GDR in  $^{197}\text{Au}$  from Ref [1, 3]. The graph shows the typical rapid fall-off of the Gauss curve as compared to the others. While Breit-Wigner and Lorentz forms do not appear too different the investigation presented in this paper shows that the Breit-Wigner curve better describes the dipole strength distribution in nuclei.

Figure 2

Comparison of the excitation factor  $f(E_x)$  as defined in Eq. I-7 for inelastic electron scattering and photon absorption. While the momentum transfer change connected with varying excitation energy is considerably lower in ( $e, e'$ ), the figure demonstrates that the effect on the cross section is comparable. The line  $f(E_x) = 1.0$  would mean that the B-value distribution and the resulting cross section are of identical shape.

Figure 3

This figure demonstrates that the dependence of the width  $\Gamma = 4.75 (E_x/E_0)^2$  MeV of the GDR on excitation energy derived from results in different nuclei [1, 11] does not describe the dipole state in one nucleus, because it is not in agreement with the experimental data.

Figure 4

Comparison of a one line Lorentz and a one line Breit-Wigner line shape fit for the ( $\gamma, n$ ) data of Veysi  re et al. [3] from  $^{197}\text{Au}$ . The left side shows the fit of either line to the cross section, while the right side corresponds to a fit with this line shapes to the B-value distribution (strength function).

The figure shows the marked improvement in  $\chi^2$  for either line shape if the excitation factor defined in equation I-7 is introduced. It also shows that the Breit-Wigner shape describes the B-value distribution better than the Lorentz shape.

The Gauss line shape resulted in  $\chi^2 > 30$  with and without excitation factor and is not shown.

Figure 5

Comparison of various fits for  $^{197}\text{Au} (\gamma, n)$ . The upper half shows the Lorentz, the lower the Breit-Wigner form. The two plots at the left are a two line fit to the cross section ( $f(E_x) = 1$ ) while the plots in the middle are fits to the B-value distribution ( $f(x) = E_x/E_0$ ; Eq. II-3). Comparison of the  $\chi^2$  as shown in the picture clearly shows that the excitation factor has to be taken into account to adequately fit the data over the full range from 10.0 - 21.7 MeV. It should be noted, that conventional evaluation of ( $\gamma, n$ ) data (Ref. 1) could only fit the range from 11 - 17 MeV. The right plots finally show that the introduction of the isovector

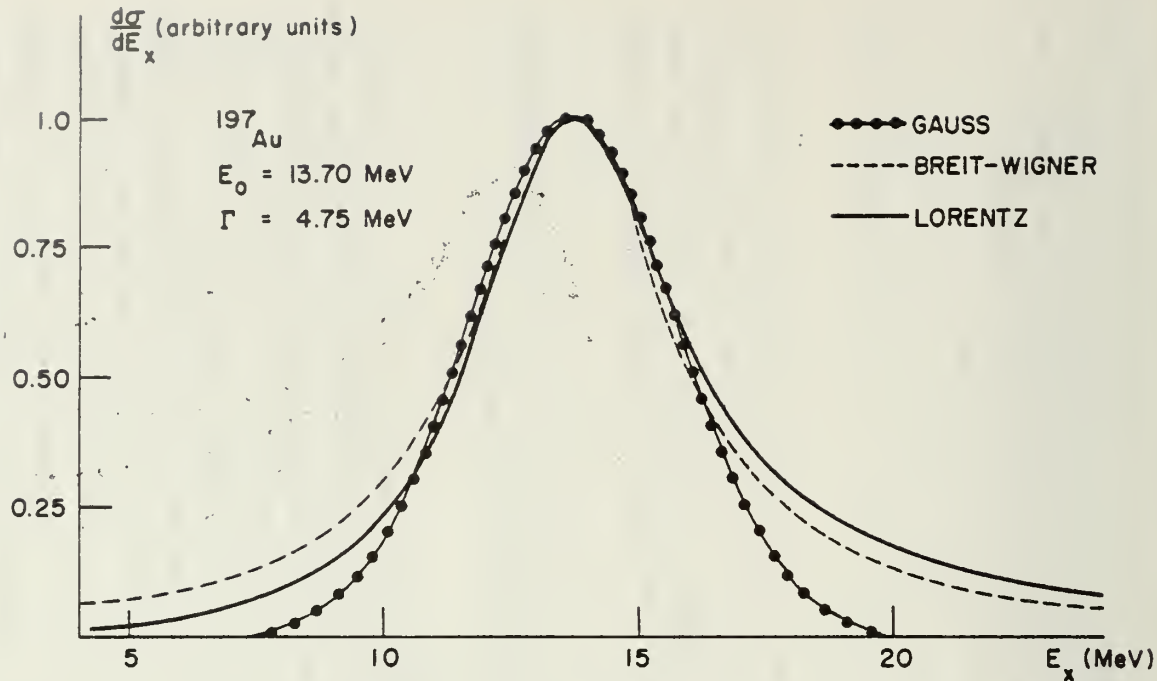


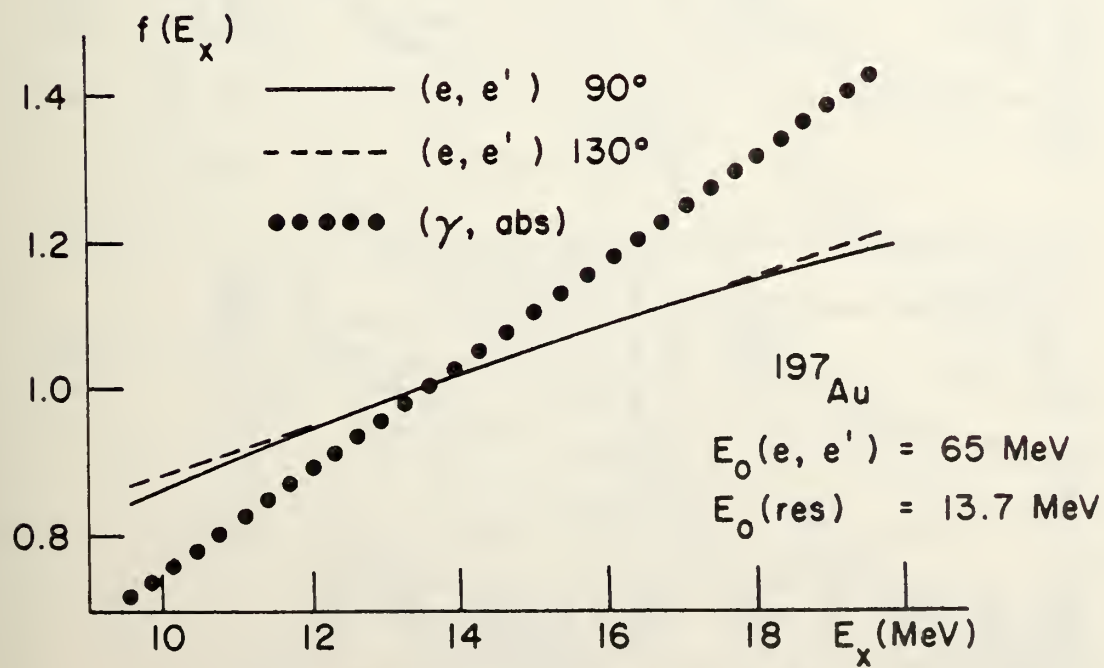
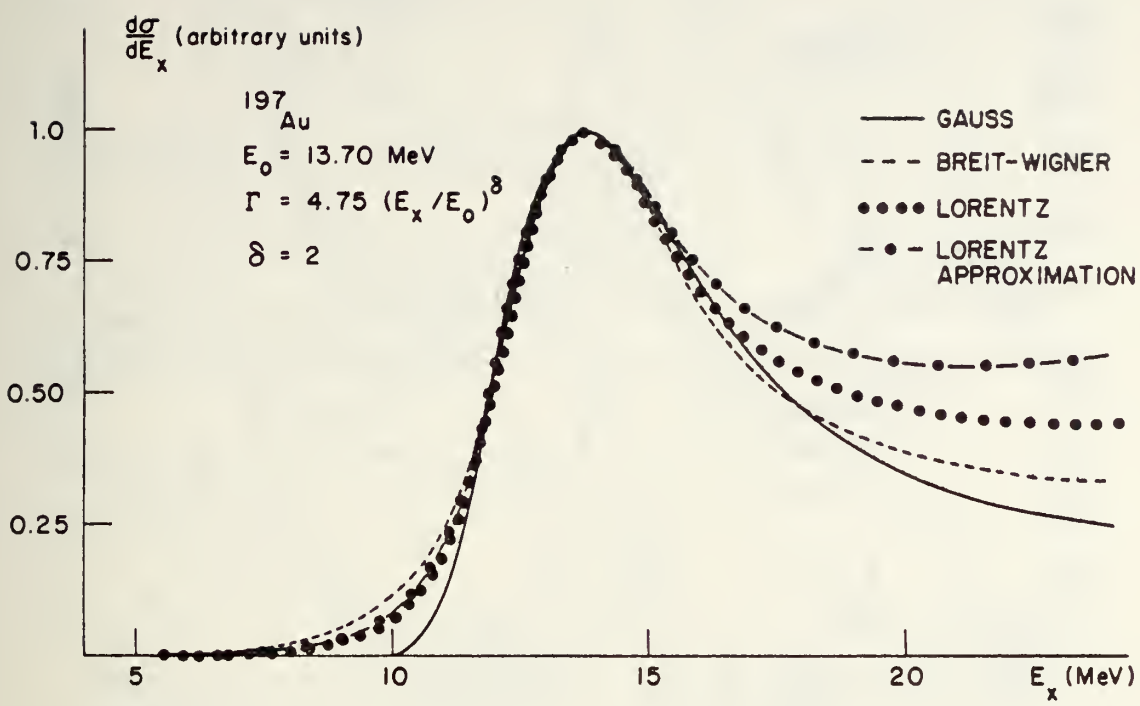
Figure 1

giant E2 resonance at 23 MeV markedly improves the  $\chi^2$ . The variance in  $\chi^2$  is 0.15. Together with figure 4, figure 5 shows that  $^{197}\text{Au}$  as to be regarded as a deformed nucleus at 14 MeV excitation energy.

Figure 6  
Similar to figure 4 and 5, but for  $^{165}\text{Ho}$ . Due to the interdependence of the two branches of the GDR the difference in  $\chi^2$  between Breit-Wigner and Lorentz form is not quite as pronounced as in  $^{197}\text{Au}$  (Figure 5) or  $^{141}\text{Pr}$  (Figure 7), but the improvement in  $\chi^2$  when fitting the B-value distribution (right part of figure) instead of the cross section is considerable.

Figure 7  
Similar to Figure 7, but for  $^{141}\text{Pr}$ . In the case of this spherical nucleus, where only one line is expected to fit the GDR the importance of the selection of the right line shape is most pronounced.

Figure 8  
Dependence of  $\chi^2$  on the parameter  $\alpha$  for the energy dependence as defined in Eq. III-2. The graph shows that, as one would expect, the  $\chi^2$  parabola has a small width.



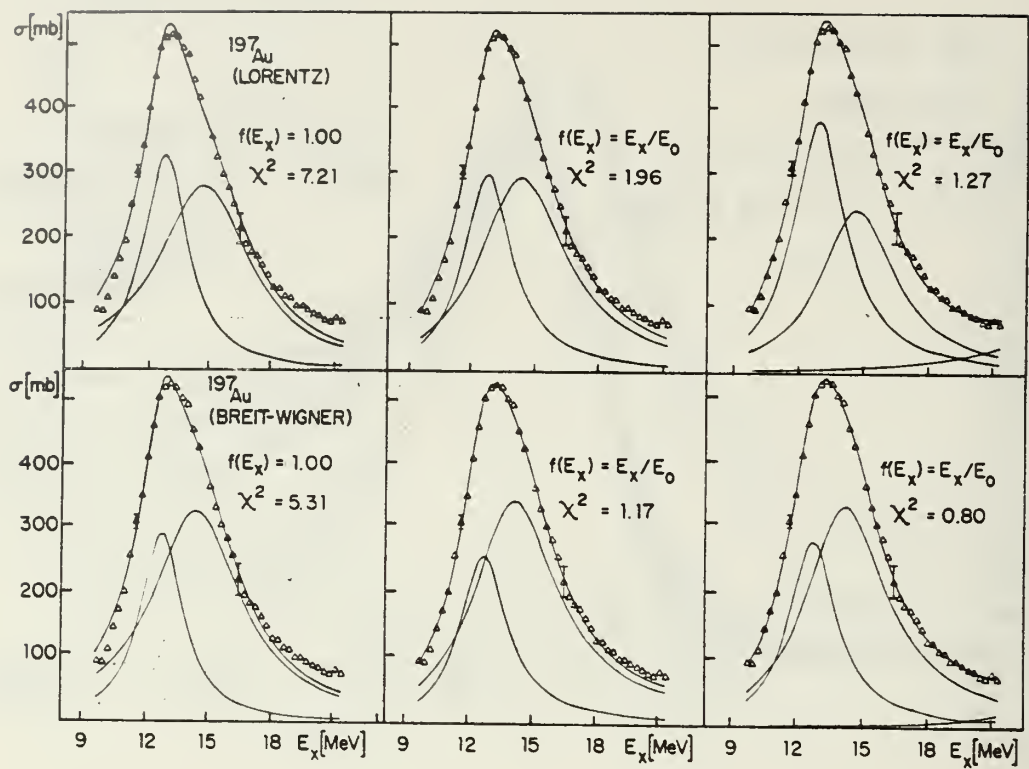


Figure 5

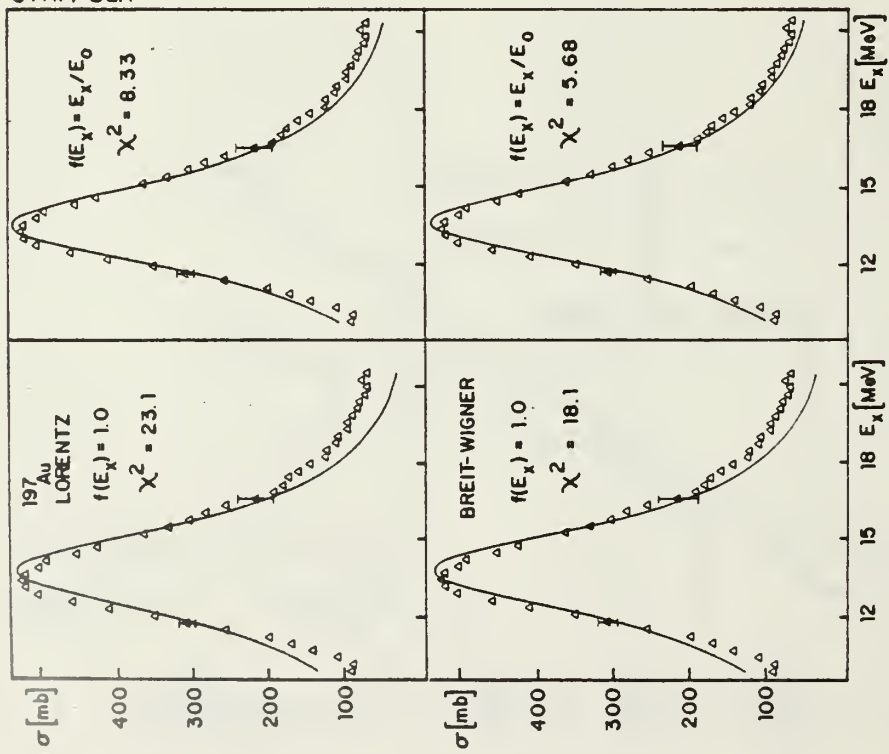


Figure 4

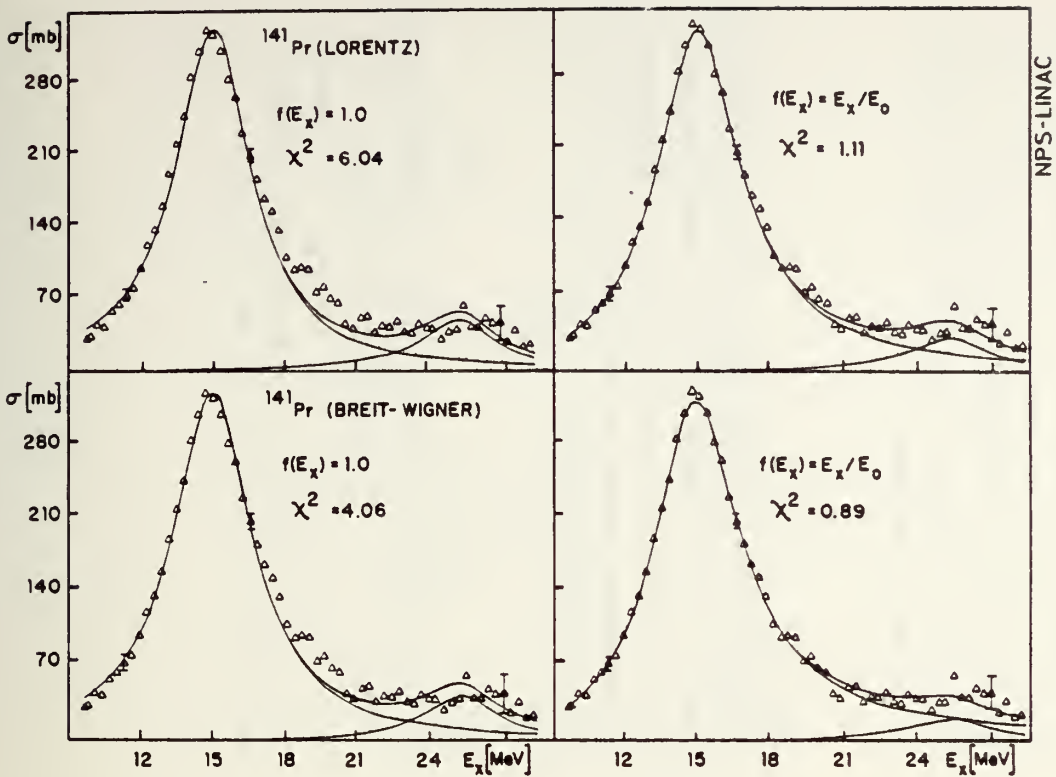


Figure 7

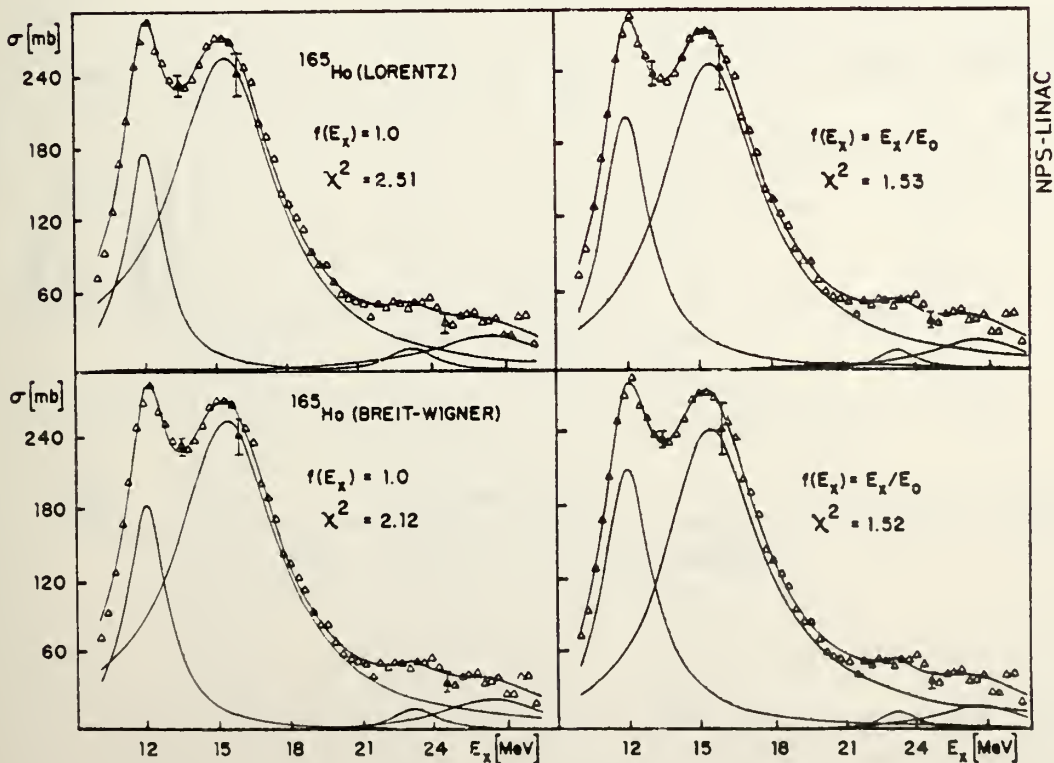


Figure 6

Table 1.

Numerical results from various fits for  $^{165}\text{Ho}$  (deformed),  $^{197}\text{Au}$  (dynamically deformed) and  $^{141}\text{Pr}$  (spherical). The resulting cross sections turn out to be consistently lower than that given in the original ( $\gamma, n$ ) measurement, thus indicating an inadequacy of the fitting method employed so far for photon experiments.

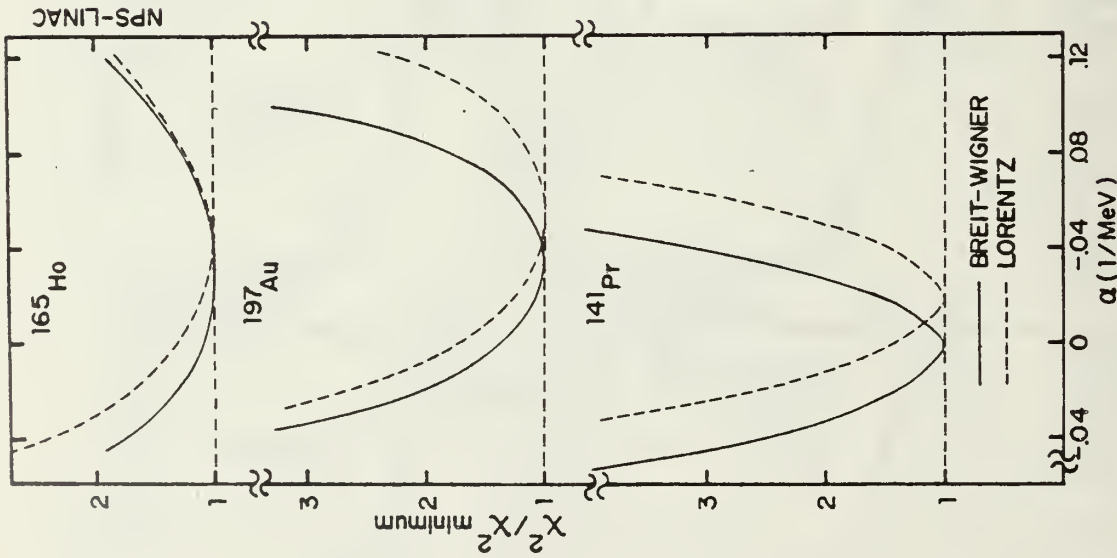


Figure 8

Table 2.

Comparison of the integrated cross sections for  $^{197}\text{Au}$ ,  $^{165}\text{Ho}$  and  $^{141}\text{Pr}$  as evaluated in this work as compared to the ( $e, e'$ ) data of Ref [15,17,18].  $^{141}\text{Pr}$  and  $^{165}\text{Ho}$  show excellent agreement, reasons for the discrepancy in  $^{197}\text{Au}$  have been given in Ref. [18].

Table 3.

This table shows the strong dependence of width and integrated strength from the assumed value for the dependence of  $\Gamma$  on  $E_x$  for  $^{141}\text{Pr}$  [ $\Gamma(E_x) = (1 + \alpha(E_x - E_0))\Gamma_0$ ].  $\alpha = 0$  results in the lowest  $\chi^2$  (Figure 8) and in the best agreement for the isovector E2 resonance at 24 MeV in ( $e, e'$ ) and ( $\gamma, n$ ).

Table II

TRK Sum Rule Exhaustion ( $\frac{1}{2}$ )		B Value (fm $^2$ )	
	( $\gamma$ , abs)	(e, e')	( $\gamma$ , abs)
Au	129	200 (Ref. 18)	65.7
Ho	106	105 (Ref. 17)	43.9
Pr	109	116 (Ref. 15)	35.2
			37.6 (Ref. 15)

Table I

Element & Line Shape	$E_0$ (MeV)	$\Gamma$ (MeV)	Peak Height (mb)	Area (MeV-mb)	$\chi^2$	Fitting Interval (MeV)	Fig.
Au - BW	13.58 $\pm$ 0.03	4.43 $\pm$ 0.09	544	3790	5.68	10.0 - 21.7	5
Au - Lor	13.62 $\pm$ 0.02	4.50 $\pm$ 0.06	542	3830	8.33	10.0 - 21.7	5
Au - BW	12.93 $\pm$ 0.09	2.72 $\pm$ 0.38	263	1120	1.17	10.0 - 21.7	6
	14.25 $\pm$ 0.22	4.65 $\pm$ 0.10	347	2530			
Au - Lor	13.03 $\pm$ 0.04	2.84 $\pm$ 0.20	311	1390	1.96	10.0 - 21.7	6
	14.48 $\pm$ 0.16	4.86 $\pm$ 0.08	305	2330			
Au - BW	12.93 $\pm$ 0.08	2.71 $\pm$ 0.30	283	1200	0.80*	10.0 - 21.7	6
	14.32 $\pm$ 0.22	4.64 $\pm$ 0.12	336	2450			
	23.00	7.00	23	250			
Au - Lor	13.08 $\pm$ 0.04	3.01 $\pm$ 0.10	388	1830	1.27	10.0 - 21.7	6
	14.80 $\pm$ 0.14	4.28 $\pm$ 0.14	249	1680			
	23.00	7.00	46	510			
Ho - BW	12.24 $\pm$ 0.02	2.31 $\pm$ 0.08	216	783	1.52*	10.4 - 29.0	7
	15.59 $\pm$ 0.04	4.51 $\pm$ 0.12	247	1750			
	23.50	1.9 $\pm$ 1.2	15	45			
	26.75	4.1 $\pm$ 2.2	21	133			
Ho - Lor	12.24 $\pm$ 0.01	2.21 $\pm$ 0.04	208	722	1.53	10.4 - 29.0	7
	15.56 $\pm$ 0.02	4.69 $\pm$ 0.07	250	1840			
	23.50	1.99 $\pm$ 0.60	17	52			
	26.75	4.6 $\pm$ 1.1	25	180			
Pr - BW	15.00 $\pm$ 0.02	4.20 $\pm$ 0.04	322	2120	0.89*	9.5 - 29.9	8
	25.60	4.00	21	135			
Pr - Lor	15.04 $\pm$ 0.01	4.11 $\pm$ 0.02	324	2090	1.11	9.5 - 29.9	8
	25.60	4.00	32	200			

## LIST OF REFERENCES

1. Berman, B. L. and Fultz, S. C., Rev. Mod. Phys., 47, 713 (1975).
2. Auerbach, N. and Yeverechyahu, A., Ann. Phys. (N.Y.) 95, 35 (1975).
3. Veyssi  re, A., Beil, H., Berg  re, R., Carlos, P. and L  pr  tre, A., Nucl. Phys. A159, 561 (1970).
4. Danos, M. and Greiner, W., Phys. Lett. 8, 113 (1964); Phys. Rev. 134, B824 (1964).
5. Danos, M. and Greiner, W., Phys. Rev. 138, B876 (1965).
6. Isabelle, D. B. and Bishop, G. R., Nucl. Phys. 45, 209 (1963).
7. Bohr, A. and Mottelson, B., Nuclear Structure, Vol. 2, (Benjamin, Reading, Mass., 1975).
8. Goldhaber, M. and Teller, E., Phys. Rev. 74, 1046 (1948).
9. Danos, M. and Fuller, E., Ann. Rev. Nucl. Sci. 15, 29 (1965).
10. Huber, M., Danos, M., Weber, H. and Greiner, W., Phys. Rev. 155, 1073 (1967).
11. Carlos, P., Berg  re, R., Beil, H., L  pr  tre, A. and Veyssi  re, A., Nucl. Phys. A219, 61 (1974).
12. Dover, C., Lemmer, R. and Hahne, F., Ann. Phys. 70, 458 (1972).
13. Ambler, E., Fuller, E. and Marshak, H., Phys. Rev. 138B, 117 (1965).
14. Br  mblett, R. L., Caldwell, J. T., Berman, B. L., Harvey, R. R. and Fultz, S. C., Phys. Rev. 148, 1198 (1966).

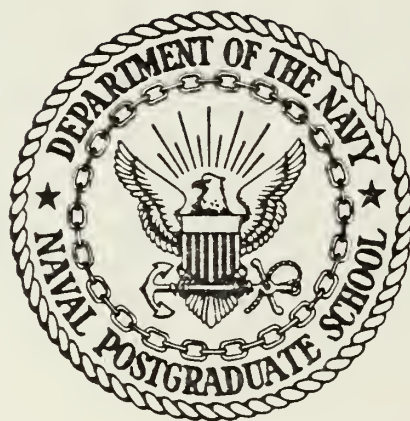
Table III

$\alpha$ (1/MeV)	$E_0$ (MeV)	$\Gamma$ (MeV)	Peak height (mb)	Area (E1) (MeV-mb)	Area (E2) (MeV-mb)
- 0.06	15.26	3.85	332	2000	260
- 0.04	15.17	3.94	330	2040	220
- 0.02	15.08	4.06	327	2080	180
0.00	15.00	4.20	322	2120	135
0.02	14.90	4.38	316	2170	80
0.04	14.80	4.61	308	2230	17
0.06	14.69	4.84	296	2250	27

15. Pitthan, R., *Z. Phys.* 260, 283 (1973).
16. Serman, B. L., Kelley, M. A., Bramblett, R. L., Caldwell, J. T., Davis, H. S. and Fultz, S. C., *Phys. Rev.* 185, 1576 (1969).
17. Moore, G. L., Buskirk, F. R., Dally, E. B., Dyer, J. N., Maruyama, X. K. and Pitthan, R., *Z. Naturforsch.* 31a, 668 (1976).
18. Pitthan, R., Buskirk, F. R., Dally, E. B., Dyer, J. N. and Maruyama, X. K., *Phys. Rev. Lett.* 33, 849 (1974); 34, 848 (1975).
19. Levinger, J. S., Nuclear Photo-Disintegration (Oxford University, London, 1960).
20. Danos, M., *Nucl. Phys.* 5, 23 (1958).

# NAVAL POSTGRADUATE SCHOOL

## Monterey, California



The Isospin of the Fine Structure between 8 and 12 MeV  
in  $^{208}\text{Pb}$  and its Implication for the Multipole  
Assignment of the 8.9 MeV Resonance<sup>+</sup>

R. Pitthan and F.R. Buskirk  
Department of Physics and Chemistry

<sup>+</sup>Supported by the National Science Foundation and  
and the Naval Postgraduate School Research Foundation

The excitation region between 8 and 12 MeV has been subject to an increasing number of investigations in recent years. This has been mainly due to the appearance of fine structure within or on top of the giant isoscalar quadrupole resonance ( $\Delta T = 0$ , E2) which is, for heavy nuclei, unique to  $^{208}\text{Pb}$ , and which structure may, therefore, contain important information concerning nuclear dynamics. However, the results

have been controversial and apparently contradictory. In this paper, we propose a solution based on a new analysis of the ( $e, e'$ ) data of Ref. 1 and a discussion of recently published ( $e, e'$ ) data of Ref. 1 and a discussion of recently published results from other experiments. The main new point is that the E2 fine structure lines near 10.6 MeV ( $\Gamma < 400$  keV) are regarded to have an isospin different from that of the underlying broad E2 resonance ( $\Gamma = 2600$  keV). Thus, because the lines and resonances differ in the iso-spin quantum number, it is justified to disentangle the different contributions by a line shape fit. Our evaluation attempts to reconcile existing controversial results. The understanding of the fine structure additionally offers a new basis for a discussion of the nature of the 8.9 MeV resonance. Throughout this paper the words 'line' and 'resonance' are used only as defined above.

The Giant Resonance Region between 8 and 12 MeV measured by ( $e, e'$ ) in  $^{208}\text{Pb}$  is disentangled into narrow lines ( $\Gamma_{\text{nat}} < 400$  keV) and broad resonances ( $\Gamma_{\text{nat}} > 1800$  keV). The narrow lines at 10.07, 10.60 and 11.37 MeV have an E2 angular distribution, and assumption of  $\Delta T=1$  for them explains controversial experimental results of electromagnetic and hadronic experiments. The new analysis makes an assignment for the 8.9 MeV resonance other than monopole difficult to understand.

In the above mentioned ( $e, e'$ ) experiment a triplet of  $2^+$  or  $0^+$  states at 10.2, 10.6, and 11.2 MeV was reported<sup>1</sup>. A

strength of 35 per cent of the energy weighted isoscalar sum rule for quadrupole excitations<sup>2</sup> (in the following abbreviated 0.35 EWSR ( $E2, \Delta T=0$ )), was found in the energy span from 9.7 to 11.7 MeV<sup>1</sup>. The small value of the strength has often been misinterpreted, because it was overlooked that this value corresponded to the cross section in the energy range from 9.7 to 11.7 MeV, and not, the total area under a resonance. Multipolarities other than E2 were ruled out by identifying fine structure in  $(\gamma, n)$ <sup>3,4</sup> with this triplet. The total structure was regarded to be the  $\Delta T=0$  GQR which had just been found in heavy nuclei<sup>5</sup>. A fourth peak at 8.9 MeV with properties similar to the members of the triplet was not evaluated because it had no counterpart in the  $(\gamma, n)$  cross section. It was stated that the E2 strength of the  $(\gamma, n)$  cross section was a factor of 2 to 5 larger than the  $(e, e')$  results. This deviation was used later by Nagao and Torizuka<sup>6</sup> as an argument against the E2 assignment for the  $(\gamma, n)$  fine structure. By evaluating the center parts of the  $(e, e')$  fine structure lines they found, however, that the  $(e, e')$  form factor had the momentum transfer dependence of an E2 transition and included little E1 strength. The E2 strength extracted for the region of the triplet by these authors was also 0.35 EWSR ( $E2, \Delta T=0$ ); the transition at 8.9 MeV followed an E2 or E0 form factor and had a strength of 0.08 EWSR (E2,  $\Delta T=0$ ).

A new argument was introduced when, on the basis of new and old  $(e, e')$  experiments, it was stated<sup>7</sup> that the narrow 8.9 MeV line should show up in  $(\gamma, n)$  at least as strong as the 10.2 MeV state, if both were E2 as reported by Nagao and Torizuka<sup>6</sup>, and that the absence of the former could be explained most easily by a monopole assignment. The width of the 8.9 MeV resonance was found to be 1.8 MeV and, assuming the same multipolarity for both line and resonance structures, the strength  $(0.50 \pm 0.25$  EWSR) ( $E0, \Delta=0$ ) or  $(0.30 \pm 0.15$  ( $E2, \Delta T=0$ )). Results of a high  $\tau^*$  solution  $(e, e')$  experiment<sup>8</sup> confirmed the strength obtained earlier<sup>7</sup> for the broad 8.9 MeV resonance, but, within the statistical limitations, showed no fine structure in this region. Thus, the arguments which had been used for a monopole assignment in this energy range must be revised. Our new evaluation shows, in contrast to Nagao and Torizuka<sup>6</sup>, that the 8.9 MeV region contains lines of various multipoles. This may also explain why the high resolution  $(e, e')$  spectrum<sup>8</sup>, which had low momentum transfer, revealed no fine structure at this energy within the limits of statistics.

We have dealt above in such detail with the  $(e, e')$  experiments because we will use electroexcitation as the basis on which to compare the results of other experiments. Electron scattering at low momentum transfer excites isoscalar and isovector transitions for E0 and E2 and the isovector E1 transition. High

multipolarities are excited only weakly. Experiments using  $(\alpha, \alpha')$  are more selective and excite only  $E_A, \Delta T=0$  transitions.<sup>9</sup> In a noncoincidence experiment,  $(e, e')$  does not show interference between excitations to states of different multipolarity<sup>10</sup>, in contrast to the  $(\gamma, n)$  reaction for which interference occurs if the differential cross section is measured by detecting the ejected neutron.

In recent high resolution  $(\gamma, n)$  investigations by Sherman et al.,<sup>11</sup> narrow transitions at 9.034, 9.421, and 10.06 MeV with a natural width of 45, 104, and 134 keV, respectively, were seen, but none of the resonant structure appeared. The lines were assumed, but not independently determined to be E2. On this basis, E2 strengths of 0.15, 0.25, and 0.48 EWSR ( $E_2, \Delta T=0$ ), respectively, were extracted.<sup>11</sup> These transitions, thus, would result in peaks more than 5 times as high as the strongest visible ones in Fig. 1 of Ref. 8, an apparent contradiction.

A  $(p, p')$  and a  $(^3He, ^3He')$  experiment<sup>12</sup> with a resolution equal to the resolution of Ref. 8, 35 keV, reports a monopole transition at 9.1 MeV with a strength of 0.02 EWSR ( $E_0, \Delta T=0$ ). It was stated by the authors<sup>12</sup> that this result is not in contradiction with the  $(e, e')$  spectra of Ref. 8. It has been pointed out by Halbert et al.<sup>13</sup> that the extraction of electromagnetic sum rule strength with inelastic hadron scattering is model

dependent. This is especially true for the monopole, where models can not be tested on low-lying collective states as can be done for other multipolarities.

Inelastic alpha scattering by Youngblood et al.<sup>9</sup> gives a width of 2.6 MeV and a strength of 0.93 EWSR ( $E_2, \Delta T=0$ ) for the resonance at 10.8 MeV, which is in very good agreement with  $(e, e')$ , and shows no monopole contribution is present in this  $(e, e')$  region. However, although their resolution, 120 keV, is better than that of Ref. 1, 200 keV, their spectra do not show the triplet structure seen in electron scattering. Inelastic proton scattering by Beirtrand and Kocher<sup>14</sup> reports a strength of 0.90 EWSR ( $E_2, \Delta T=0$ ) for a resonance at 10.6 MeV, but shows neither a resonance nor a line at 8.9 MeV. The fine structure around 10.5 MeV reported earlier<sup>15</sup> was not seen again, but a prominent 'line' of either E2 or E3 character was found at 9.4 MeV.

The most serious shortcoming of all previous experiments is that the fine structure was never separately evaluated in a way which would establish its multipolarity directly from angular distributions. In the evaluation, the narrow lines were always put together with the underlying resonances or simply assumed to be E2. This is a crucial point, because, e.g., an E1 ( $\Delta T=1$ ) assignment for the fine structure alone could qualitatively explain why it is seen in  $(\gamma, n)$  and  $(e, e')$ ,

but not in  $(\alpha, \alpha')$ , while on the other hand, it would be such a small fraction of the total strength that the E2 angular distribution would not be noticeably affected. In order to overcome this shortcoming and to do an analysis which is consistent with  $(\alpha, \alpha')$ , we have resolved the strength function into fine structure, referred to as lines, and broad resonances<sup>16</sup>. In the present analysis the  $(e, e')$  spectrum  $s(E_x)$ , where  $E_x$  is the excitation energy, is fitted<sup>17</sup> to a function of the form:

$$f(E_x) = a + bE_x + cR(E_x) + \sum g_i(E_x). \quad (1)$$

The first two terms represent the background.  $R(E_x)$  is the radiation tail function, which accounts for energy loss by bremsstrahlung in the target, radiation during scattering, energy straggling and ionization. Both of the radiation terms contain the elastic electron scattering cross section, which is calculated from a phase shift analysis. Each line or resonance is represented by a spectral function  $g_i(E_x)$ . The strength function  $B_i(E_\lambda, E_x)$ , which determines  $g_i(E_x)$ , is assumed to have a Breit-Wigner form with appropriate constants for the resonance energy, width and height. In the fitting program, the constants  $a, b$  and  $c$  are varied, and the various constants for the resonances may be fixed or varied depending on the information known about the given resonance. Cri-

teria for a good fit are a low value of  $\chi^2$ , no significant deviation of  $f$  from  $s$  (which would indicate an omitted resonance) and consistent values for a resonance energy and width when the several spectra for different angles or beam energies are considered together. As a check for reliability it should be noted that  $a$  is in agreement with the value expected from the measurement of the constant room background (target-in), that  $b$  is a small correction and that  $c$  is close to one, indicating that essentially no scaling of the radiation tail is necessary.

For the present analysis of  $^{208}\text{Pb}$ , the known excitation energy and width, but not the strength for the  $E2^9$  resonance were used as fixed parameters in the fit. Figure 1 shows a fit to a spectrum of Ref. 1 under these assumptions. The angular distributions for the broad resonances at 10.8 MeV and 8.9 MeV are only consistent with E2 or E0 assignments. The total widths and EWSR fractions are given in Table 1. The energy weighted sum rule for the quadrupole ( $\lambda=2$ ) strength is given by<sup>18</sup>

$$S(E_\lambda) = \frac{\hbar^2}{2M_p} \frac{\lambda(2\lambda+1)^2}{4\pi} Z e^2 \langle r_p^{2\lambda-2} \rangle_0,$$

with fractions  $Z/A$  and  $N/Z$  assigned to the isoscalar and isovector modes, respectively. For the isoscalar monopole mode, the sum rule due to Ferrell<sup>19, 20</sup> is used:

$$E_x \cdot |M_{fi}|^2 = \frac{\hbar}{M} \cdot Z \langle r_p^2 \rangle_0.$$

The three lines of the triplet similarly follow an E2 (E0) angular distribution, but their combined strength is surprisingly small (less than 0.1 EWSR, see Table 1). Figure 2 compares the experimental results for the 10.07 Mev line with DWBA calculations based on the Tassie (Goldhaber-Teller) model<sup>2</sup>. It is directly evident from the figure that the main part of the ( $e, e'$ ) cross section is definitely not of E1 character. As an upper limit of the E1 strength, a reduced transition probability of  $B(E1) = 0.3 \text{ fm}^2$  can be given, which is 30 per cent less than the E1 strength seen by Sherman et al.<sup>11</sup> at 10.06 MeV. The angular distribution of the 8.91 MeV line on top of the 8.9 MeV resonance indicates a transverse contribution in addition to an E1 or E2 state.

43

These contradictory results from various experiments can be reconciled if one assumes an E2,  $\Delta T=1$  assignment for the three lines at 10.07, 10.60, and 11.37 MeV, but not for the line at 8.91 MeV, which may even not be E2:

1. A  $\Delta T = 1$  state will not, or only very weakly, be excited by  $(\alpha, \alpha)$ , because the alpha particle has  $T = 0$ . It could be excited by inelastically scattered particles with  $T \neq 0$ , as in  $(p, p')$ <sup>14</sup>, but the strength is expected to be suppressed by a factor of 10 as compared to isoscalar excitations.

2. If the triplet seen in  $(\gamma, n)^4$  does in fact correspond to the  $(e, e')$  fine structure, the difference in strength noted earlier<sup>1</sup> would have to be explained. Possibly the  $(\gamma, n)$  fine structure can be enhanced by an interference

between the E2 lines and the tail of the GDR. Such interference has recently been observed in measurements of the differential  $(\gamma, n)$  cross section<sup>22</sup>. Thus, one has to assume that E1-E2 interference in the  $(\gamma, n)$  reactions takes place with the  $\Delta T = 1$  part of the E2 strength (lines), but not with the  $\Delta T = 0$  part (resonance). Since the GDR is isovector in nature, such an assumption seems plausible. The appearance of the lines in the older integrated  $(\gamma, n)$  measurements<sup>4</sup> then would only be possible if the  $(\gamma, n)$  detector did not have a  $4\pi$  geometry, which is the case.

3. The difference in total width between the 10.8 MeV ( $E2, \Delta T=0$ ) resonance and ( $E2, \Delta T=1$ ) fine structure may be attributed to the different decay channels available to different isospin states.

4. A  $\Delta T = 1$  assignment for the lines is consistent with calculations by Ring and Speth<sup>23</sup> who report on  $\Delta T = 1$  contributions to the predominantly  $\Delta T = 0$  transitions around 11 MeV. It is clear from the excitation energy that these lines cannot be analogue states. Since  $\Delta T = 1$  states at this excitation energy can only decay through admixture of  $\Delta T=0$  impurities their natural width offers a unique possibility to study this admixture. The  $\Delta T = 1$  strength of the three lines together (Table 1) is close to the value  $((N-Z)/A)^2$  derived from a simple mass oscillation model for the ratio of iso-vector and isoscalar sums by Halbert et al.<sup>13</sup> but falls short by a factor of four to their value calculated with microscopic

wave functions.

The foregoing explains in a consistent manner the results from various experiments for the E2 resonance at 10.6 MeV and the fine structure in this region. The problem of the nature of the resonance at 8.9 MeV must be treated separately as we do below.

A resonance structure at  $53 \text{ A}^{-1/3}$  MeV, compatible with either E2 or E0 multipolarity, has been seen for several years<sup>7, 8, 24, 25</sup>. An E0 assignment is favored over E2 by the following arguments:

1. An E2( $\Delta T=0$ ) resonance at this energy with 0.35 EWSR ( $E2, \Delta T=0$ ) (Table 1) leads to a total strength of 1.48 EWSR ( $E2, \Delta T=0$ ) to which the known states at 4.07, 6.20, and 10.8 MeV contribute 0.17, 0.06, and 0.86 EWSR, respectively. A total strength this large would be difficult to understand for the isoscalar sum, where no exchange terms enter<sup>2</sup>. In addition to the sum rule argument, an E2 resonance of 0.35 EWSR ( $E2, \Delta T=0$ ) should lead to a visible resonance in the hadronic scattering experiments<sup>9, 14</sup>. Assumption of E0 explains why it has not been seen.
2. Assumption of E2 ( $\Delta T=1$ ) for the 8.9 MeV resonance would explain why it is absent in the hadronic spectrum, but poses the problem of explaining why a broad resonance of  $\Delta T=1$  character should appear several Mev below the narrow  $\Delta T=1$  triplet.

3. The energy for the E0 breathing mode, calculated by "uberal"<sup>26</sup> from optical isotope shifts, agrees with the observed 8.9 MeV. The isotope shift yields a compressibility parameter  $K = (81 + 61 - 25)$  MeV, which is related to the monopole energy by  $E = 0.95 \sqrt{K^{-2}}$ , giving  $(8.6 + 2.7 - 1.5)$  MeV.

Recently monopole strength  $> 1.0$  EWSR ( $E0, \Delta T = 0$ ) has been proposed (see Ref. 28 and References therein) from a very weak resonance at about  $80A^{-1/3}$  MeV. Such a resonance would be superimposed on the GDR, which in electron scattering would yield a peak almost twice as high as the GDR shown in Figure 1. Thus, there is no possibility to accommodate a monopole state stronger than about 0.1 EWSR ( $E0, \Delta T = 0$ ) in the present ( $e, e'$ ) data, especially if one realizes that for the momentum transfer covered (Figure 2), the E2 relative cross section is at a maximum compared to the E1. The arguments of Ref. 28 (and the References quoted therein) are based solely on the assumption that  $(\alpha, \alpha')$  and  $(d, d')$  do not excite the isovector GDR at all. This may not be true. In turn then, the cross-section of the resonance at  $80A^{-1/3}$  MeV as seen in  $(\alpha, \alpha')$  and  $(d, d')$ , interpreted as E1, might be very suited to investigate the role of isospin impurities. We would also like to point out that the arguments given in favor of E0 over E2 at 14 MeV in the last paragraph of Ref. 28 apply equally to the assignment of E0 vs. E2 for the 8.9 MeV resonance. Finally, it should be noted that the small structure at 14 MeV in Figure 1 would be compatible with the 0.2 EWSR ( $E4, \Delta T = 0$ ) offered as a further alternative assignment in Ref. 28.

It is a pleasure to thank P. Axel, W. Benenson, B. Berman, A. Bohr, B. Mottelson, N. Sherman, and D. Youngblood for critical discussions and helpful remarks. We are especially obliged to Th. Walcher for his many valuable suggestions.

Figure 1:

Reanalysis of a spectrum of 64.6 Mev electrons, scattered inelastically at  $93^\circ$  from  $^{208}\text{Pb}$  with an overall resolution of 190 kev in the giant resonance region. The statistical error is smaller than the size of the experimental points. The triplet around 10.6 Mev is but a small fraction of the cross section. In addition to the states mentioned in the text one has to take into account lines at 7.4, 7.9, 8.4, and 9.4 Mev. More structure is visible at 12 and 14 Mev. The excitation energies of the freely fitted resonances,  $(8.9 \pm 0.2)$  Mev (E0),  $(13.6 \pm 0.2)$  Mev (E1), and  $(18.5 \pm 0.9)$  Mev (E3) denotes the maxima of the strength functions, not of the cross sections. It should especially be noted that the strength found for the E1 resonance,  $B(E1) = 60 \text{ fm}^2$ , is in essential agreement with the  $(\gamma, n)$  values of  $55 \text{ fm}^2$  and  $75 \text{ fm}^2$  from Ref. 3 and Ref. 4, respectively.

Figure 2:

Ratio of the inelastic cross section to the Mott cross section for the narrow line at 10.07 Mev. The curves show DWBA calculations for a primary energy of 64.6 Mev and an excitation energy of 10.07 Mev. The method of Ziegler and Peterson (Phys. Rev. 165 1337 (1968)) was used to display points from measurements with different primary energies in the same drawing.<sup>46a</sup> Only measurements with scattering angle smaller than  $130^\circ$  were used to avoid transverse contributions.

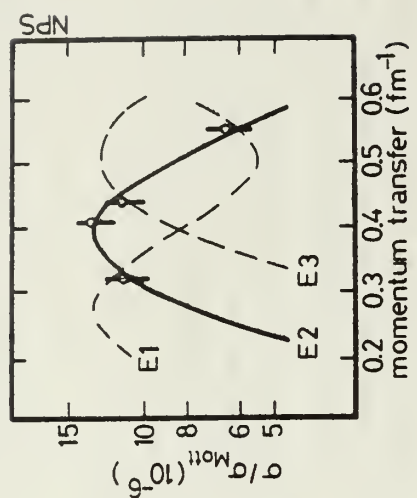


Figure 2

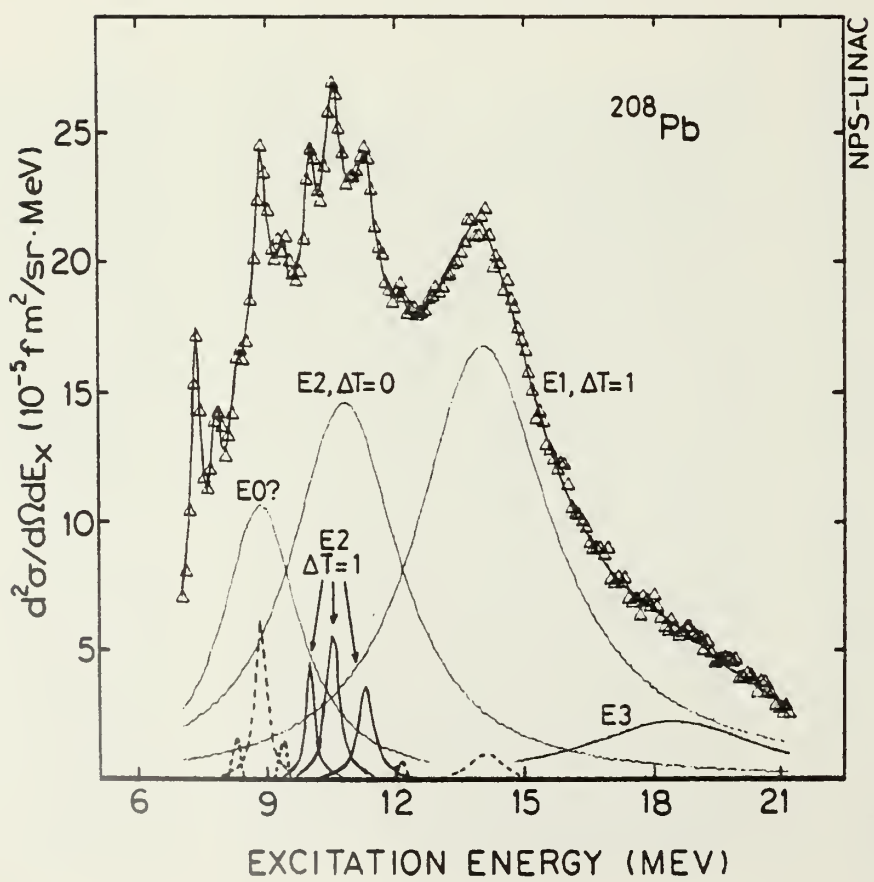


Figure 1

$E_x$ (MeV)	$\Gamma$ (MeV)	$\lambda^{\pi}, \Delta T$	$R^a$	$B(E\lambda) (fm^4)$
10.07 $\pm$ 0.03	0.20 $\pm$ 0.05	2+, 1	0.013	150 $\pm$ 30
10.60 $\pm$ 0.04	0.32 $\pm$ 0.06	2+, 1	0.025	280 $\pm$ 40
11.37 $\pm$ 0.05	0.37 $\pm$ 0.05	2+, 1	0.019	200 $\pm$ 40

- a)  $R = B(E\lambda, \Delta T) E_x / EWSR(E\lambda, \Delta T)$
- b) The values from Youngblood et al.<sup>9</sup> were used in order to achieve a fit compatible with the ( $\alpha, \alpha'$ ) experiments.

The rms ground state radius of Friar and Negele (Nucl. Phys. A212, 92 (1973)) was used to calculate the E2- and E0 sum rules. The widths but not the strengths

of the lines depend on the line shape used; a Breit-Wigner form was found to give the best fit. Multiplying the E2 sum rule by 1.34 gives the equivalent monopole sum rule for each state; the 8.9 MeV monopole state interpreted as E2, thus, corresponds to 0.35 EWSR (E2,  $\Delta T = 0$ ). Isoscalar and isovector sums differ by the factor (N/z).

Table 1

References:

1. F.R. Buskirk, H.D. Graf, R. Pitthan, H. Theissen, O. Titze, and Th. Walcher, Phys. Lett. 42B, 194 (1972).
2. A. Bohr and B.R. Mottelson, Nuclear Structure, Vol. II, p. 403 (Benjamin, New York, 1975).
3. B.L. Berman and S.C. Pultz, Rev. Mod. Phys. 47, 713 (1975);  
B.L. Berman, Atlas of photoneutron Cross Sections (Bicentennial Edition, 1976), UCRL-78482.
4. A. Veyssiére, H. Beil, R. Bergerie, P. Carlos and A. Leprette, Nucl. Phys. A159, 561 (1970).
5. R. Pitthan and Th. Walcher, Phys. Lett. 36B, 563 (1971); Z Naturforsch. 27a, 1683 (1972).
6. M. Nagao and Y. Torizuka, Phys. Rev. Lett. 30, 1068 (1973).
7. R. Pitthan, F.R. Buskirk, E.B. Dally, J.N. Dyer, and X.K. Maryama, Phys. Rev. Lett. 33, 849 (1974); 34, 848 (1974).
8. A. Schwiercinski, R. Frey, A. Richter, E. Spamer, H. Theissen, O. Titze, Th. Walcher, S. Krewald, and S. Rosenfelder, Phys. Rev. Lett. 35, 1244 (1975).
9. D.H. Youngblood, J.M. Ross, C.M. Rosza, J.D. Bronson, A.D. Bacher, and D.R. Brown, Phys. Rev. C13, 994 (1976), and private communication.
10. D. Drechsler and H. Überall, Phys. Rev. 181, 1383 (1969).
11. N.K. Sherman, H.M. Ferdinand, K.H. Lokan, and C.K. Ross, Phys. Rev. Lett. 35, 1215 (1975), and private communication.
12. H.P. Morsch, P. Decowski, and W. Benenson, Phys. Rev. Lett. 37, 263 (1976).
13. E.C. Halbert, J.B. McGroarty, G.R. Satchler, and J. Speth, Nucl. Phys. A245, 189 (1975).
14. F.E. Bertrand and D.C. Kocher, Phys. Rev. C13, 2241 (1976).
15. M.B. Lewis, F.E. Bertrand, and D.J. Horen, Phys. Rev. C8, 389 (1973).
16. R. Pitthan and F.R. Buskirk, Bull. Am. Phys. Soc. 21, 516 (1976).
17. F.R. Buskirk and R. Pitthan, Bull. Am. Phys. Soc. 21, 683 (1976), and to be published
18. E.K. Warburton and J. Weeneser in Isospin in Nuclear Physics, ed. by D.H. Wilkinson (North Holland, Amsterdam, 1969).
19. R.A. Ferrell, Phys. Rev. 107, 1631 (1957).
20. S. Fukuda and Y. Torizuka, Phys. Rev. Lett. 29, 1109 (1972).
21. S.T. Tuan, L.E. Wright, and D.S. Onley, Nucl. Instrum. Methods 60, 70 (1968).
22. P.A. Russo, P.A. Dickey, J.R. Calarco, and P. Axel, Bull. Am. Phys. Soc. 20, 629 (1975) and private communication.
23. P. Ring and J. Speth, Nucl. Phys. A235, 315 (1974).
24. R. Pitthan and Th. Walcher, Z. Naturforsch. 27a, 1683 (1972).
25. R. Pitthan, Z. Physik 260, 283 (1973).
26. H. Überall, Electron Scattering from Complex Nuclei, (Academic Press, New York, 1971)
27. J.D. Walecka, Phys. Rev. 126, 653 (1962).
28. M.N. Harakeh, K. van der Borg, T. Ishimatsu, H.P. Morsch, A. van der Woude, and F.E. Bertrand, Phys. Rev. Lett. 38, 676 (1977).

# NAVAL POSTGRADUATE SCHOOL

## Monterey, California



Giant Resonances and Bound Collective States Observed  
in the Scattering of 92.5 MeV Electrons from the  
Closed Neutron Shell Nucleus  $^{89}\text{Y}$  between Excitation  
Energies from 2 to 55 MeV\*

R. Pitthan, F.R. Buskirk, E.B. Dally<sup>+</sup>, J.O. Shannon,  
and W.H. Smith

Department of Physics and Chemistry

Work supported by the National Science Foundation and the Naval Postgraduate School Research Foundation

<sup>+</sup>Now at Varian Associates, Palo Alto California 94303

ABSTRACT

92.5 MeV electrons were used to study in  $^{99}\text{Y}$  the excitation range between 2 and 55 MeV. Above neutron threshold, broad electric resonances have been seen at 14.0 ( $6.3\text{A}^{-1/3}$ ) MeV ( $E1, \Delta T = 1$ ) and 28 ( $1.25\text{A}^{-1/3}$ ) MeV ( $E2, \Delta T = 1$ ). The total width of the isoscalar E2 resonance is  $(4.5 \pm 0.4)$  MeV and its strength  $(56 \pm 6)\%$  EWSR ( $E2, \Delta T = 0$ ). For the isovector E2 resonance only a minimal value of 7 MeV for the width can be given which is connected with  $(48 \pm 5)\%$  of the isovector sum rule. The strength of the E1 resonance [ $T_{\epsilon}, (104 \pm 10)\%$  of the Thomas-Kuhn-Reiche sum rule] agrees well with  $(\gamma, n)$  measurements, thus giving a check for the accuracy of the evaluating methods employed. A structure around 19 - 20 MeV, believed to be the  $T_{\epsilon}$  part of the GDR, carries  $(8 \pm 3)\%$  of the E1 sum rule. In addition to these generally well known states, clustering of E3 strength,  $(13 \pm 2)\%$  EWSR ( $E3, \Delta T = 1$ ), was found at 6.75 and 8.05 MeV; the enveloping line shape of these clusters was best described by a Breit-Wigner term. Other concentrations of strength include E3 at 2.6 MeV,  $(15 \pm 3)\%$  EWSR ( $E3, \Delta T = 0$ ), E2 at 4.0 MeV,  $(11 \pm 3)\%$  EWSR ( $E2, \Delta T = 0$ ) and E3 strength at 13.5 MeV. No resonance other than the E1 was found around 17 MeV, thus ruling out in  $^{99}\text{Y}$  the existence of a monopole state with 100% sum rule proposed for  $^{90}\text{Zr}$  from  $(\alpha, \alpha')$  and  $(e, e')$  measurements. In contrast to heavy nuclei, no resonant  $3\hbar\omega$  E3 strength could be located.

I. INTRODUCTION

Nuclei with closed shells have played an important role in the discovery of Giant Resonances other than the Dipole Resonance.<sup>1</sup> The "new" (isoscalar) E2 state, for example, was found to be of identical width in the  $N = 82$  nuclei  $^{140}\text{La}$ ,  $^{140}\text{Ce}$ , and  $^{141}\text{Pr}$  before even the multipolarity or other properties were established with certainty.<sup>2</sup> The importance of the closed shell nuclei rests mainly with the fact that the continuum states have relatively small width, typically of the order of 3 MeV, and can therefore be recognized as resonant structures above the radiative  $(e, e')$  or nuclear  $(p, p')$  background.

A comparison between nuclei in the  $^{200}\text{Pb}$  ( $N = 126, Z = 82$ ), and the  $^{140}\text{Ce}$  ( $N = 82$ ) region<sup>3</sup> and the  $^{90}\text{Zr}$  ( $N = 50$ ) region<sup>4</sup> shows one fundamental difference. The ratio  $R$  of the width of the GQR,  $\Gamma_{E2'}$ , to the width of the GDR  $\Gamma_{E1}$  in the heavier nuclei is 0.65 to 0.75, but found to be 1.1 to 1.2 in  $^{90}\text{Zr}$ . Since  $^{90}\text{Zr}$  is the only nucleus for which  $R > 1$  has been reported, we thought it important to investigate the  $N = 50$  nucleus  $^{99}\text{Y}$ . It is reasonable to expect, and in fact borne out by the experiments carried out so far, nearly identical gross properties of the giant resonances in neighboring spherical nuclei.

Besides the question of the width of the otherwise well known E2 ( $\Delta T = 0$ ) state (see, e.g., Ref. 6) there is the much less well known isovector ( $\Delta T = 1$ ) Giant Quadrupole resonance.<sup>7</sup> The latter is important for testing microscopic theories of collective excitations, but not too much is known over a wide

variety of nuclei. Because it lies high in excitation energy, it easily exhausts the appropriate energy weighted sum rule. The great width of these states, typically 7 MeV, makes the experiments the more difficult. Experiments require very good statistics and reliable knowledge of general and radiative background. Since much of our effort in the last two years went into improving just this knowledge we felt confident to be able to make more definitive statements about the strength and location of the E2 ( $\Delta T = 1$ ) state in medium heavy nuclei than have been possible in the past.

Other unsolved problems in  $N = 50$  nuclei include the magnetic states, a proposed monopole state at 17 MeV,<sup>1</sup> exactly under the giant dipole resonance, and higher multipoles. The range of momentum transfer  $q$  was chosen not only to include the maxima of the E2 and E3 form factors but also to allow the analysis of E1 and E4 transitions. Figure 1 shows arbitrarily normalized cross sections for various multipolarities. They were calculated with a DWBA program using transition charge and current distributions peaking at the nuclear surface (Tassie model, see below). It is evident from Figure 1 that a distinction between, e.g., M2 and E3 from the momentum transfer dependence alone is not easily possible. Since we, however, have restricted our measurements to forward angles, magnetic states other than M1 would have to exhaust several times the sum rule strength to show up noticeably.

## II. EXPERIMENTAL DETAILS

Electron scattering spectra were obtained at the Naval Postgraduate School linear accelerator laboratory. Self-supporting targets with thicknesses between 110 and 180 mg/cm<sup>2</sup> were used. The scattering angles were 75°, 90°, 105° and 120° at a constant elastic energy of 92.5 MeV. The corresponding momentum transfer  $q$  ranged from 0.54 to 0.76 fm<sup>-1</sup> for an excitation energy of 10 MeV.

The 120 MeV NPS LINAC consists of three S-band sections, driven by separate 20 MW klystrons. The repetition rate is 60 or 120 sec<sup>-1</sup>, depending on energy, and the duty cycle is about 0.0001. Maximum average current at a resolution of 300 kev is 2  $\mu$ A. The deflection system consists of two 30° sector magnets and two quadrupole doublets, in an achromatic system designed by K. L. Brown.<sup>10</sup> The 16" spectrometer is 120°, and double focusing. All power supplies are regulated to better than 1 part in 10<sup>4</sup>. The beam spot on the target is less than 1 mm in diameter and extremely stable and reproducible.

The spectrometer does not have an open back and produces, therefore, an appreciable ghost peak. This peak is superimposed on any inelastic scattering spectrum, at a point where the magnetic field is low enough so that the numerous elastically scattered electrons hit the inside of the spectrometer chamber and scatter indirectly into the counters. In our spectrometer the ghost peak appears at an energy of 92% of that of the elastic peak, is known through measurements in <sup>12</sup>C and can thus be accounted for in the evaluation, although this

introduces an additional uncertainty for the cross sections in the 7 to 8 Mev region at forward angles.

The scattered electrons are finally detected in a 10 counter ladder in the focal plane of the spectrometer. The detector system consists of the 10 front counters and two backscattering counters arranged in 10 triple coincidence channels. The beam is limited to a value such that the accidental coincidence rate is always lower than 5%.

Due to the location of the accelerator, the target chamber is close to the deflection area. The difficulties associated with a relatively high background have been overcome by a very good overall beam stability backed by a system which only accepts counts if the beam intensity is within 10% of a preset value.

Also the beam monitor deserves comment. Usually a Faraday cup is employed, which produces high background if located near the target or extra focusing if far away. The NPS LINAC employs a five foil sealed secondary emission monitor located near the target. The background produced is low, it intercepts all the beam, and frequent comparison with a Faraday cup, which is removed during experiment, showed that the efficiency is stable to one part in  $10^{-8}$ .

A fair overall description of our experimental setup would be: A conventional design, but through tedious work well adopted to our major scientific interest; measurements of "not so well known" giant resonances.

### III. EVALUATION

#### A. Principles

The inelastic scattering spectra were measured relative to the elastic cross sections. The latter were evaluated using the phase-shift code of Fischer and Rawitscher.<sup>11</sup> Although this is a relatively old program, comparison with a more recent one<sup>12</sup> showed that the results are in agreement of better than 0.5% with the latter. The charge distribution parameters

$c = 4.86 \text{ fm}$  and  $t = 2.38 \text{ fm}$  were taken from the work of Fivozinski, et al.<sup>13</sup> The elastic, but not the inelastic, cross sections were corrected for Swinger and Bremsstrahlung corrections.<sup>14</sup>

Three different kinds of background contribute to the observed inelastic spectra. The first is the general room background measured with "target-out," which in our case is small, due to the directional coincidence applied in the counting system, and very constant over time, i.e., independent of the tuning of the machine. The second is the "target-in" background which consists mainly of electrons which are originally scattered by the target but which penetrate the counter shielding or undergo subsequent scattering in the walls of the spectrometer. The third type of background is the elastic radiation tail which is caused by photon emission before, during and after scattering and additional energy straggling and ionization. While conventional wisdom knows that the radiation tail (RT) cannot be calculated exactly enough in heavy nuclei, our results show that in fact it can. The progress made in this

direction is described elsewhere<sup>15</sup>; here we only want to note that we are able to describe our total background as a function of energy  $E_f$  of the outgoing electron between 5 and 40 Mev excitation energy by the formula:

$$\text{BGR}(E_f) = P_1 + P_2 \cdot \frac{1}{E_f} + P_3 \cdot R^T$$

This expression for BGR is incorporated in a line shape fitting routine with the  $P_i$  being fitted parameters. While  $P_1$  is close to the value expected from the accidental coincidence rate,  $P_2$  turns out to be small and  $P_3$  is close to one, thus leaving the radiation tail essentially unchanged. To be able to appreciate the improvement of this form with only three free fitting parameters against an often employed heuristic polynomial background fit, one must know that in our case the latter would require a polynomial of 6th to 9th order in  $E_f$  to fit the radiation tail function alone. Thus the heuristic polynomial fit is inadequate. If a low order polynomial were used, the radiation tail could not be fit, a high order polynomial, however, would make the background selection arbitrary.

The line shape fitting procedure as such has been described in detail by Pitthan,<sup>16</sup> who also gives the reasons why one should not apply the radiative corrections to the giant resonance cross sections. All the resonances and clusters of states evaluated in this paper were found to be best described by a Breit-Wigner line shape for the B-value distribution

(strength function)

$$\frac{dB}{dE_X} = \left| \frac{\frac{dB}{dE_X}}{(E_X - E_0)^2 + (\Gamma/2)^2} \right|_{\max}$$

with  $E_X$  being the excitation energy,  $\Gamma = \text{FWHM}$ , and  $E_0$  the (excitation) energy of the maximum of the strength function.

There are some slight but important differences between the shape of the strength function and the cross section of the resonances which have been described by Pitthan<sup>16</sup> and more recently, in greater detail, by Gordon, et al.<sup>17</sup> The resonance energies and widths given in this paper are those of the strength function and not those of the cross section, because the latter depends on primary energy and scattering angle, while the first does not. In accord with common practice, a best fit was determined when a minimum in chi-square  $\chi^2$  was found.  $\chi^2$  is defined as

$$\chi^2 = \sum^n (x_i - x_o)^2 / \sigma^2$$

$(x_i$  calculated value of cross section,  $x_o$  measured value of the cross section,  $\sigma$  standard deviation associated with  $x_i$ ).

Related to this  $\chi^2$  distribution is the term degrees of freedom, defined as the number of experimental points (typically of the order 400, i.e., 10 per MeV) minus the number of parameters fitted (24, i.e., 3 for each of the seven Breit-Wigner Lines used plus 3 for the background). The expected theoretical value for  $\chi^2$  (per degree of freedom) in our case is  $\chi^2_{\text{theory}} = 1.00 \pm 0.08$ . Due to an interpolation process used to assemble the sum spectrum from the 10 counter ladder, our data points are not totally statistically independent and  $\chi^2$  is decreased by about 20%.

A resonance has to fulfill the following criteria before it is accepted in our evaluation. Its inclusion into the fit

has to be necessary for a  $\chi^2 < 1$  and consistent values of position, width and strength must be obtained for the several spectra taken at different momentum transfer.

Naturally there are other methods of evaluation possible.

Instead of a line shape fit, Fukuda and Torizuka<sup>6</sup> have recently employed a model dependent so-called "multipole expansion" for re-evaluating their giant resonance data.<sup>5</sup> This method would correspond to fitting a four term Fourier series (E1 to E4) to five points (number of spectra taken). Further, it does away with one of the valuable advantages of (e,e'), the possibility of a nearly model independent<sup>10</sup> analysis of (e,e') cross sections. Moreover, it also gives away one of the most beautiful features of giant resonances in medium heavy and heavy nuclei, namely the existence of coherent resonant states in the continuum instead of just humps, lumps and bumps of various multiplicities.

By the same token, with our method we will not be able to detect strength which is fairly evenly distributed over the continuum as one may suspect for E4 and higher multipoles, due to the many shell model states available to them.

#### B. B-Values and Sum Rules

The method of extracting B-values from (e,e') in heavy nuclei where the Born approximation is no longer valid has been described most clearly by Ziegler and Peterson.<sup>10</sup>

In Born approximation the B-value is defined for a nucleus with ground state spin  $\alpha$  by the formula for the relative cross section:

$$\sigma/\sigma_{\text{Mott}} = 4\pi/c^2 (2\lambda + 1) \left| \int j_\lambda(qr) g_{\text{tr}}(r) r^2 dr \right|^2$$

and the reduced transition probability

$$B(E\lambda) = (2\lambda + 1) \left| \int r^\lambda g_{\text{tr}}(r) r^2 dr \right|^2.$$

The second integral may be regarded as the first term of a power series development of the Bessel function under the first integral.

The cross sections (area A under the resonance) used in this paper were calculated from the fitting parameters by  $A = (\pi/2\Gamma \cdot \text{Height})$ , i.e., they correspond to the resonance integrated from  $-\infty$  to  $+\infty$ .

Other units for transition strength beside the B-values are ground state radiation width  $\Gamma_Y^0$  (eV), single particle units (SPU) and percentages of sum rule strength. For the results of this work the following formulas were used:

$$\Gamma_Y^0 = \frac{8\pi\alpha}{T(2\lambda + 1)^2} \frac{\lambda + 1}{\lambda} \frac{E_X^{2\lambda+1}}{(hc)^2} ; \quad R_0 = 1.2A^{-1/3} ; \quad (\text{Ref. } 19)$$

$$B(E\lambda)_{\text{SPU}} = \frac{2\lambda + 1}{4\pi} \left( \frac{3R_0\lambda}{\lambda + 3} \right)^2 ; \quad R_0 = 1.2A^{-1/3} ; \quad (\text{Ref. } 19)$$

$$S(E\lambda, \lambda > 1) = E_X \cdot B(E\lambda) = \frac{2\lambda(2\lambda + 1)^2 h^2}{8\pi M} < R^{2\lambda-2} >; \quad (\text{Ref. } 20)$$

$$S(E1) = E_X \cdot B(E1) = \frac{9h^2}{8\pi M} \frac{NZ}{A} ; \quad (\text{Ref. } 21)$$

( $\alpha = 1/137$ ,  $M_f$  monopole matrix element,  $M$  proton mass).

Concerning the division of strength between isoscalar ( $\Delta T = 0$ ) and isovector ( $\Delta T = 1$ ) modes for  $\lambda = 0$  and  $\lambda > 1$  the

usual assumption was made that a fraction Z/A goes into the isoscalar excitation and the remaining strength N/A goes into the isovector part. Since this division is based on the validity of the hydrodynamical model (surface oscillations), it poses only a problem for the monopole excitation, where the role of the excess neutrons is unclear. The momenta  $\langle R^{2n} \rangle$  used in the sum rule calculation were determined by numerical integration of the ground state charge distribution as measured by  $(e, e')$ .<sup>13</sup> With the thus calculated  $\langle R^2 \rangle = 18.2 \text{ fm}^2$  and  $\langle R^4 \rangle = 452 \text{ fm}^4$ , the full EWSRs for  ${}^{19}\text{Y}$  have the values

$$E_x \cdot B(E2) = 5.86 \cdot 10^4 \text{ MeV fm}^4 \text{ and } E_x \cdot B(E3) = 4.28 \cdot 10^6 \text{ MeV fm}^6.$$

U<sub>1</sub>

#### IV. RESULTS

##### A. General

Figure 2 shows a spectrum of 92.5 Mev electrons scattered under 105° from  ${}^{19}\text{Y}$ . The spectrum has not been modified in any way, e.g., the dispersion correction has not been applied. The background drawn does not correspond to the real background; it is only intended to guide the eye. Several distinct features are apparent without a detailed analysis: (1) Lines with relatively small width at 2.5 and 4 MeV; (2) a doublet of lines at 7 and 8 MeV; (3) two wider resonances at 14 and 17 MeV and; (4) a very wide state at 28 MeV. Numerical analysis reveals that there are less strong resonances at 10.5 and 13.5 and possibly at 20 and 24 MeV. Since the one at 20 MeV was noticeable only at 75° and 90° where, according to Figure 1, the E1, as compared to other multipoles, is at a relative maximum, we concluded it to be the T<sub>2</sub> part of the GDR. In contrast, the structure at 24 MeV shows up only at 105° and 120°. If taken to be real, it would be compatible with a strength of 208 of the isoscalar E3 EWSR.

From the known systematics of the GR one would suspect that the resonances around  $14(63A^{-1/3})$  MeV,  $17(76A^{-1/3})$  MeV and  $28(125A^{-1/3})$  MeV are the E2 ( $\Delta T = 0$ ), E1 ( $\Delta T = 1$ ) and E2 ( $\Delta T = 1$ ) GR, respectively. A look at Figure 1 and Figure 3 again verifies this idea: The change in peak height of the 14 and 17 MeV resonances between 90° and 120° as shown in Figure 3 corresponds to the relative change in cross section as shown in Figure 1.

All lines drawn in Figure 3 and 4 had to be included in spectra from at least 3 angles to achieve a reasonable  $\chi^2$ . Omission of any one of them makes a consistent fit of all spectra and a  $\chi^2$  (per degree of freedom)  $\leq 1$  impossible.

#### B. The Giant Dipole Resonance and the Breathing Mode

The GDR, the prominent feature in photo nuclear reactions, has been extensively measured in  $^{99}\text{Y}$  with quasi monochromatic photons.<sup>22, 23</sup> From the  $(\gamma, n)$  cross sections one may, for a certain multipolarity, calculate the equivalent B-value by the formula<sup>24</sup>

$$\int \sigma_\gamma dE_\gamma = 16\pi^2 \hbar c a \frac{\lambda+1}{\lambda} \frac{1}{[(2\lambda+1)!!]^2} k^{2\lambda-1} B(E_\lambda, k)$$

with  $a = 1/137$ ,  $\lambda$  multipolarity and  $k = E_\lambda/\hbar c$ .

The values thus calculated from  $(\gamma, n)$  are given in Table 1 together with other available results in  $N = 50$  nuclei. The results presented here were obtained by comparing DWBA cross sections,<sup>25</sup> calculated using the Tassie model,<sup>26</sup> (which leads to the same transition charge as the Goldhaber-Teller<sup>27</sup> model) with the experimental cross sections. Frequently the Steinwedel-Jensen<sup>28</sup> model is preferred for isovector resonances. However, the G-T (Tassie) model with its simple dependence on the radius,

$$\rho_{\text{tr}}^G(r) = C_G r^{\lambda-1} d\phi_0(r)/dr$$

consistently describes the El results in medium and heavy nuclei better than the S-J model and is therefore also used here. Figure 5 shows the Goldhaber-Teller DWBA cross sections compared with our result. We also have drawn the Steinwedel-

Jensen cross section, calculated with the transition charge density

$$\rho_{\text{tr}}^S(r) = C_S r^\lambda d\phi_0(r)/dr$$

inserted into the DWBA program of Tuan et al.<sup>25</sup> As

apparent from Figure 5, the Steinwedel-Jensen model, when fitted to the  $(e, e')$  data, fails to describe the cross section at the photon point (average from Refs. 22 and 23) by a factor of two, while the Goldhaber-Teller model is in quite good agreement.

In our forward angle spectra we see a systematic deviation between 19 and 20 MeV excitation energy and in fact the insertion of a resonance improves the 75° and 90° fits. Figure 6 shows, with an extended scale, the region between 12 and 24 MeV at an angle of 90°, which shows both structures. As mentioned above, we identified the structure at ~20 MeV with the  $T_>$  part of the GDR.<sup>29</sup> If we do so, we find  $(8 \pm 3)\%$  of the El sum rule, in reasonable agreement with the value found in  $^{90}\text{Zr}$ .<sup>30</sup> To summarize the results for the El resonance, we finally note that the  $T_<$  El strength found exhausts all of the strength predicted by  $(\gamma, n)$  measurements and dipole sum rule and that the strength and momentum transfer dependence is well described by the Goldhaber-Teller model.

These results are important in judging the merits of two proposals<sup>31, 32</sup>, which put the monopole breathing mode at 17 MeV in  $^{90}\text{Zr}$ . While  $^{99}\text{Y}$  is in principle a different nucleus and the resonances might be totally different in the two nuclei,

in practice this seems to be highly improbable. Furthermore, the similarity of the electric giant resonances for neighboring nuclei has been demonstrated for  $\text{La}$ ,  $\text{Ce}$  and  $\text{Pr}$ .<sup>2,16</sup> In order to shed some light on this important problem we have calculated the  $(e, e')$  cross sections corresponding to  $100\%$  EWSR ( $E_0, \Delta T = 0$ ) for an E0 resonance at 17 MeV with a width of 4 MeV as proposed recently for  $^{90}\text{Zr}$ .<sup>8</sup> The result is drawn with a broken line into Figure 7. It is important to note that we used the monopole program of the Sendai group,<sup>11</sup> for the calculation. It is evident from this figure that there is not enough cross section to accommodate  $100\%$  EWSR. From our fits we may set an upper limit of  $10\%$  E0 EWSR at 17 MeV. Thus, even the existence of a resonance with approximately  $20\%$  EWSR ( $E_0, \Delta T = 0$ ) at 17 MeV as proposed by Marty et al.<sup>9</sup> for  $^{90}\text{Zr}$  seems not very likely. Finally, we would like to mention that the disagreement gets worse, if one uses the Steinwedel-Jensen model for the E1 as in Ref. 8.

### C. The Isoscalar Giant Quadrupole Resonance

The observation of strong broad resonances in  $(e, e')$ <sup>2,12</sup> at an excitation energy of  $63A^{-1}/^3\text{MeV}$  just below the GDR has brought about a renewed interest in the general properties in the nuclear continuum. A multitude of experiments has produced a wealth of information.<sup>3,13</sup> The overall features of position and strength of the GQR in nuclei with  $A > 40$  are well understood from both macroscopic<sup>3,14</sup> and microscopic<sup>15</sup> theories. Discrepancies between strength observed with various experimental methods for nuclei with  $A < 40$  seem to be understood.<sup>3,16</sup> The

reason why we studied  $N = 50$  nuclei is the difference in width between E2 and E1 resonances of  $^{90}\text{Zr}$ <sup>5</sup> compared to  $^{160}\text{Ce}$ <sup>16</sup> or  $^{208}\text{Pb}$ .<sup>3</sup> There are no microscopic theories which explain the width of giant resonances. A macroscopic approach using the concept of viscosity and the hydro-dynamic model shows an overall agreement with the trend of the data as a function of nuclear mass, but does not account for shell effects.<sup>17</sup> Calculations for the effect of a deformed potential on the five sublevels of an E2 state<sup>18</sup> describe the broadening in the deformed nucleus  $^{165}\text{Ho}$ <sup>19</sup> quantitatively. Figure 8 shows that the resonance we find at 14.0 MeV with a width of  $(4.5 \pm 0.4)$  MeV follows an E2 DWBA cross section. Compared with other experiments, Table 2 shows that only the excitation energies are in reasonable agreement in all of them. The most pronounced discrepancy is with the scattering of 155 MeV protons.<sup>20</sup> However, a systematic comparison with other available data shows that in all nuclei investigated, the half width and the strength of the E2 state from Ref. 40 is smaller than results from other experiments.

The width from  $(\alpha, \alpha')$  scattering<sup>1</sup> is smaller than the width we find. It has been pointed out<sup>21</sup> that because the  $\alpha$ -particle is relatively slow, the decay time of the resonance and the travel time of the  $\alpha$  in the nucleus are of the same order of magnitude. Rearrangement of the nucleons during that time could therefore influence the observed width. This speculation is backed by the observation<sup>6</sup> that  $\alpha$ -data are generally better fitted by a Gaussian shape than by a Lorentz or a Breit-Wigner form, while the opposite is true for electromagnetic

excitation.<sup>17</sup> Such effects should, however, not greatly influence the strength, and here our results are in excellent agreement with other experiments, except for the multipole expansion results.<sup>8</sup>

We conclude, therefore, that indeed the width of the isoscalar E2 state at  $63\text{A}^{-1/3}$  MeV is greater than the width of the higher lying E1 resonance, thus differing from results for heavier nuclei but in agreement with the viscosity model.<sup>3</sup>

#### D. The Isovector Giant Quadrupole Resonance

In contrast to the  $63\text{A}^{-1/3}$  state the E2 resonance predicted<sup>3</sup> and found<sup>9</sup> around  $130\text{A}^{-1/3}$  MeV is much less well known. The importance of both states for our understanding of nuclear dynamics has recently been emphasized.<sup>12</sup> In particular, it is important to know position, total width, and strength of both isoscalar and isovector parts of the quadrupole excitation to be able to fully test nuclear models.<sup>7</sup> Isovector resonances are only weakly (protons) or not at all ( $\alpha$ -particle) excited by hadronic scattering. The  $\Delta T = 1$  resonances are therefore mainly open to investigation by radiative capture and electron scattering.

While  $(e, e')$  does not measure isospin directly, the identification of the  $130\text{A}^{-1/3}$  resonance as the isovector E2 state is aided by theoretical arguments.<sup>1</sup> The absence of this state in  $(\alpha, \alpha')$  is indirect experimental proof that this resonance is indeed isovector in nature.<sup>6</sup>

The information available for this state has been collected by Paul.<sup>7</sup> While he found that the basic characteristics are already in evidence and that it will be difficult to learn more

about this mode, Hanna<sup>3</sup> more recently emphasized the need for more detailed  $(e, e')$  experiments to establish the existence and universal nature of the isovector E2 resonance as a coherent state.<sup>8</sup>

The  $E2, \Delta T = 1$  strength is found to exhaust approximately the full sum rule in heavy nuclei and is concentrated in a relatively small energy range (approximately 5 MeV).<sup>3</sup> It is split in deformed nuclei,<sup>9</sup> and becomes wider for light nuclei.<sup>5</sup> Depending on the evaluation method employed, its strength seems to vary between 23%<sup>4</sup> and 73%<sup>6</sup> of the EWSR in the  $N = 50$  nucleus  $^{90}\text{Zr}$ . A recent proton capture experiment using the  $^{69}\text{Y}(p, \gamma_0)^{90}\text{Zr}$  reaction finds indication for E2 (and E3) strength above the GDR on the basis of a direct-semidirect model.<sup>13</sup> When the authors used the parameters from Ref. 8 for an E2 ( $\Delta T = 1$ ) state at 26 MeV, the agreement between calculations and experiment improved, even though no structure of the cross section was found at 26 MeV. However, depending on the coupling, the E2 capture strength had to be reduced to 40% EWSR in order to be compatible with the data.<sup>13</sup>

In our spectra for  $^{69}\text{Y}$  we find a coherent resonance at 28 MeV (Figure 4). The width is difficult to extract accurately because this resonance is both high in energy and very broad. If we assume it to be 7 MeV, which is also the smallest value found to fit the data, (48 ± 5)% of the EWSR ( $E2, \Delta T = 0$ ) is concentrated in this state. This value changes to (57 ± 6)% EWSR for  $\Gamma = 8$  MeV. The maximum width which is still compatible with a  $\chi^2 < 1$  is  $\Gamma = 10$  MeV (Table 3). As described in the

next section, this difficulty may be connected with a very wide structure at 45 MeV. Comparison of DWBA and experimental cross section for  $\Gamma = 8$  MeV in Figure 9 demonstrates that this resonance is clearly of E2 character. The strength from the proton capture experiment is consistent with ours if we assume  $\Gamma = 7$  MeV to be the correct width. Comparison of the change in width from  $^{208}\text{Pb}$  to  $^{89}\text{Y}$  then would be in agreement with one prediction of the viscosity model,<sup>17</sup> namely that the isovector width will vary more slowly with A than the isoscalar width.

In summary, we believe our data to be the best available for medium heavy nuclei in statistical accuracy. They clearly show the existence of a coherent E2 state at  $125\text{A}^{-1/3}$  MeV which carries at least -45% and possibly as much as 75% of the isovector sum rule.

#### E. The E3 Strength

It has long been recognized that the low-lying octupole states in nuclei comprise only a small fraction of the energy weighted sum rule and that more strength should be expected at higher energies. In particular, the missing 1  $\hbar\omega$  strength has been predicted to lie at 5-6 MeV ( $30\text{A}^{-1/3}$  MeV) in heavy nuclei.<sup>18</sup> Indeed, such states have been found by electron scattering more than a decade ago.<sup>19</sup> A description of isoscalar and isovector strength, based on the concepts of the Bohr-Mottelson self-consistent model, has been made, among others, by Hamamoto<sup>20</sup> and is given in Table 4. Since the Shell model allows both 1  $\hbar\omega$  and 3  $\hbar\omega$  transitions for octupole excitations, the situation is more involved than in the case of quadrupole excitations for

which only 2  $\hbar\omega$  is available for transitions into high-lying states. The E3 strength is therefore more widely distributed and more difficult to locate.

The resonance found at approximately  $195\text{A}^{-1/3}$  MeV in heavy nuclei (44 MeV in  $^{89}\text{Y}$ )<sup>3,39</sup> has been recently determined to be the isovector 3  $\hbar\omega$  state.<sup>46</sup> As incentive for more experiments we would like to mention that we find systematic deviations between our data and the fitted background around 45 MeV which can be explained by a resonance about 15 MeV wide, and which possibly is responsible for the somewhat inconclusive result concerning the width of the E2 ( $\Delta T = 1$ ) state, described in the preceding section. But since there is presently no way to prove that these difficulties are not based on deficiencies of our background procedure above 40 MeV, we are not yet able to quantitatively evaluate this region.

As mentioned earlier, the fits indicated a resonance between 19 and 20 MeV at forward, and 22 and 26 MeV at backward angles. The latter is consistent with a resonance carrying  $20\%$  EWSR ( $\Delta T = 0$ , E3) and thus might be part of the ( $\Delta T = 0$ ) 3  $\hbar\omega$  E3 state. It is noticeable, however, that the E2 state at 28 MeV has a slight tendency to rise at backward angles relative to the DWBA cross section, thus possibly indicating non-resonant cross section of a high multipolarity.

We are able, however, to give more definitive results for the 1  $\hbar\omega$  strength. At 13.5 MeV (Figures 3, 4 and 6) we find an E3 state of relatively small width ( $\Gamma = 1.2$  MeV) which carries  $(2.5 \pm 0.6)\%$  EWSR (E3,  $\Delta T = 1$ ). The comparison with

DWBA calculations in Figure 11 shows this state to be of E3 character. Figure 1 shows that the only other assignment consistent with the angular distribution would be M2, which can be ruled out by strength arguments. Regarding the crudeness of Hamamoto's model<sup>15</sup>, the degree of agreement between her prediction of the strength and our result can only be called surprising, but it shows once more the conceptual correctness of the Bohr-Mottelson model.

Lower in energy, we find two groups of states centered at 6.75 and 8.05 MeV which also follow an E3 form factor (Figure 10) and carry 13% of the EWSR ( $E_3, \Delta T = 0$ ). Together with the group of states at 2.6 MeV<sup>16</sup>, they exhaust all the expected  $1 \ h\nu$  ( $\Delta T = 0$ ) strength (Table 5). It should be specifically noted that their strength weighted excitation energy of  $22A^{-1/3}$  MeV is in good agreement with the predictions.<sup>15</sup> The clusters at 7 and 8 MeV correspond to the well-known E3 states at 5.4 MeV ( $\sim 32A^{-1/3}$  MeV) in  $^{200}\text{Pb}$ <sup>16</sup> with 17%

EWSR ( $E_3, \Delta T = 0$ ). These types of states have recently been investigated more systematically with  $(\alpha, \alpha')$  in medium heavy nuclei.<sup>17</sup> There they were also found to cluster around  $32A^{-1/3}$  MeV as in  $^{200}\text{Pb}$ <sup>16</sup> and the other  $(e, e')$  experiments<sup>18</sup> and were classified as the upper part of the  $1 \ h\nu$  isoscalar strength.

In summary, we have found all the expected  $1 \ h\nu$  E3 strength in  $\pi\pi$  (isoscalar and isovector) predicted by the Shell model, but our data show only weak indication for  $3 \ h\nu$  states.

#### F. Other States

Our spectra show some other states which have been indicated in Figures 2, 3, 4 and 6 but have not been discussed so far.

At 2.6 MeV we see a structure approximately 1 MeV wide. It has E3 q-dependence and is identical with three E3 states measured with higher resolution by Fivozinski et al.<sup>19</sup> Further up in energy a state at 4.0 MeV, not yet reported in the literature, is best described by an E2 q-dependence and carries a  $B(E2) = (700 \pm 100) \ \text{fm}^4$ .

A state at 10.5 MeV could also be E2, but is better described by a mixture of M1 and E2. Since, however, we have restricted our measurements to forward angles, we cannot really disentangle E2 and M1. These backward angle measurements would have to be carried out at an accelerator with higher incident current.

#### G. Errors

The errors given are the estimated total errors, which are larger than the statistical error would be. The estimate was based on how the areas under the curves changed during the fits due to different choice of resonance parameters, background, ghost peak subtraction, etc., while still maintaining  $\chi^2 < 1$ .

V. SUMMARY

We have measured the excitation range between 2 and 55 MeV in  $^{69}\text{Y}$ . Our general aim was to search for resonant structure in the continuum. Our data are in agreement with current ideas and macroscopic and microscopic calculations. For the quadrupole excitations of the continuum, we are able to cut down the error margin by a factor of three. Our results are collected in Table 6.

The following points deserve special emphasis:

1. The isovector E2 strength is concentrated in a resonant state which comprises at least 45% of the isovector sum rule, if we use the minimum width compatible with the data (7 MeV), or as much as 75%, if we assume  $\Gamma = 10$  MeV to be correct. The problem of the width alone deserves further research.
  2. We have found an E3 state at 13.5 MeV which possibly can be identified with the E3 ( $1 \ h\nu$ )  $\Delta T = 1$  excitation.
  3. We do not see excess cross section in the region of the GDR which could accommodate the isoscalar monopole state in the strength recently proposed.
  4. Together with the low-lying states at 1.6 and 3.1 MeV (3.5% EWSR) and 4.0 MeV [ $(11 \pm 3)\%$  EWSR], we find a total of 70% EWSR for the isoscalar E2 strength in  $^{69}\text{Y}$ .
  5. In contrast to our investigations of heavy nuclei, we do not see resonant 3  $h\nu$  E3 ( $\Delta T = 0$  or  $\Delta T = 1$ ) strength.
- We would like to thank H. L. McFarland and D. D. Snyder for helping us keep the Linac running and G. M. Bates and D. H. Dubois for their help in the long hours of collecting data.

TABLE 1. Comparison of some results for the E1 (GDR) Resonance in  $N = 50$  nuclei

Ref	$E_0$ (MeV)	$\Gamma$ (MeV)	$R(8)$ a)	Meth.	Nucleus
22	16.79	$3.95 \pm 0.06$	$87 \pm 6$	$(\gamma, n)$	$^{69}\text{Y}$
23	16.74	$4.1 \pm 0.1$	$111 \pm 5$	$(\gamma, n)$	$^{69}\text{Y}$
5	16.65	4.0	$107 \pm 32$	$(e, e')$	$^{90}\text{Zr}$
8	— b)	4.0	$113 \pm 25$	$(e, e')$	$^{90}\text{Zr}$
this work	16.6	$3.9 \pm 0.2$	$104 \pm 10$	$(e, e')$	$^{69}\text{Y}$

a)  $R = E_X \cdot B(E1)/EWSR (E1, \Delta T = 1) \cdot 100$

b) the authors used the  $(\gamma, n)$  value

TABLE 2. Compilation of some results for the E2 ( $\Delta T = 0$ ) Resonance in  $N = 50$  nuclei

Ref.	$E_O$ (MeV)	$\Gamma$ (MeV)	$R(\%)^a)$	Meth.	Nucleus
5	14	$4.8 \pm 0.6$	$56 \pm 17$	(e, e')	$^{90}\text{Zr}$
6	$14.5 \pm 0.3$	$4.0 \pm 0.2$	$54 \pm 15$	( $\alpha, \alpha'$ )	$^{90}\text{Zr}$
8	14 b)	$4.5^b)$	84	(e, e')	$^{90}\text{Zr}$
40	$13.8 \pm 0.2$	3.2	$24 \pm 5$	(p, p')	$^{89}\text{Y}$
this work	$14.0 \pm 0.2$	$4.5 \pm 0.4$	$56 \pm 6^c)$	(e, e')	$^{89}\text{Y}$

a)  $R = E_X \cdot B(E2)/EWSR (\Delta T = 1, E2) \cdot 100$

a)  $R = E_X \cdot B(E2)/EWSR (\Delta T = 0, E2) \cdot 100$   
The  $\Delta T = 1$  sum rule is connected with that of Table 2 by a factor of  $N/2$

b) Values were taken from Ref. 41

c) The rms - radius  $R = 4.27$  fm of Ref. 13 was used for calculating the sum rule yielding a EWSR ( $E2, \Delta T = 0$ ) of 25800 Mev fm.

a)  $R = E_X \cdot B(E2)/EWSR (\Delta T = 1, E2) \cdot 100$

The  $\Delta T = 1$  sum rule is connected with that of Table 2 by a factor of  $N/2$

b) The value for the sum rule percentage depends on the coupling used for the model.

TABLE 4. Shell model (RPA) predictions for excitation energy and strength of the E3 transitions. The numbers were taken from Ref. 45 using  $\hbar\omega = 40A^{-1/3}$  MeV.

	CLASSIC			$\Delta T = 0$			$\Delta T = 1$			
	$E_x (\hbar\omega)$	$E_x (A^{-1/3} \text{ MeV})$	$R(\%)$	$E_x (A^{-1/3} \text{ MeV})$	$R(\%)$	a)	$E_x (A^{-1/3} \text{ MeV})$	$R(\%)$	a)	
1	40	0.14	24	0.28	52	0.02	2.6	0	12	$15.0 \pm 2.0$
3	120	0.86	105	0.72	192	0.98	6.75	0	30	$5.5 \pm 1.0$

a)  $R = E_x \cdot B(E3)/EWSR (\Delta T, E3) \cdot 100$

TABLE 5.  $1 \hbar\omega$  E3 transitions in  $^{69}\text{Y}$ . The theoretical values were taken from Hamamoto's and somewhat depend on the coupling used for the RPA calculations. One should note that the strength weighted energy for the  $\Delta T = 0$  states is  $22A^{-1/3}$  MeV, close to the predicted value.

	EXPERIMENT			THEORY		
	$E_x$ (MeV)	$\Delta T$	$E_x (A^{-1/3} \text{ MeV})$	$R(\%)$	$E_x$ (MeV)	$R(\%)$

FIGURE CAPTIONS

FIGURE 1

DWBA cross sections for E1' to E4 and M2 transitions divided by the Mott cross section. The curves were normalized so that the first maxima are equal. The program of Tuan et al.<sup>2,5</sup> was used with a transition charge density  $\rho_{tr}(r) = N_\lambda r d\varphi_0(r)/dr$  for the electric transitions and a transition current density  $j_{tr}(r) = N_\lambda d\varphi_0(r)/dr$ . The figure shows that the momentum transfer covered by this experiment is selective for multipolarities 1 to 4.

FIGURE 2

Spectrum of 92.5 Mev electrons scattered inelastically at 105°. The background does not correspond to the real background, it is only intended to guide the eye. The count rate has not been corrected for the constant momentum dispersion of the magnetic spectrometer. Note the suppressed vertical scale. Excitation energy is given in units of  $A^{-1/3}$  Mev (upper scale) and Mev (lower scale).

FIGURE 3

Spectrum of 92.5 Mev electrons scattered inelastically from  $^{99}Y$  at 90° and 120°. Note that the scale for the 90° spectrum (left scale) is not suppressed. The resonances which were used for fitting the spectra and the background as described in the text are drawn. The spectra were

$E_x$ (MeV)	$E_x (A^{-1/3} \text{ MeV})$	$T$ (MeV) <sup>a</sup>	$B$ (fm <sup>-2</sup> )	$R$ (g) <sup>b</sup>	$T_y$ (eV)	SPU	$\chi$	AT
2.6	-	$1.0 \pm 0.2$	$(1.12 \pm 0.15) \cdot 10^5$	$15 \pm 3$	$5.3 \cdot 10^{-6}$	34	3	0
4.0	-	$1.0 \pm 0.2$	$700 \pm 140$	$11 \pm 3$	$1.2 \cdot 10^{-1}$	6	2	0
6.75	30	$1.0 \pm 0.2$	$(16.5 \pm 3.0) \cdot 10^3$	$6 \pm 1$	$6 \cdot 2 \cdot 10^{-4}$	5	3	0
8.05	36	$1.2 \pm 0.2$	$(16.5 \pm 2.5) \cdot 10^3$	$7 \pm 1$	$2.1 \cdot 10^{-3}$	5	3	0
13.5	60	$1.2 \pm 0.2$	$(4.4 \pm 1.0) \cdot 10^3$	$2.5 \pm 0.6$	$2.1 \cdot 10^{-2}$	1.4	3	1
14.0	63	$4.5 \pm 0.4$	$1040 \pm 100$	$56 \pm 6$	$9.0 \cdot 10^{-1}$	8.8	2	0
16.6	74	$3.9 \pm 0.2$	$20.5 \pm 2.0$	$104 \pm 10$	$3.3 \cdot 10^4$	5.3	1	1
28.0	125	$T = 7$	$565 \pm 65$	$48 \pm 5$	$1.57 \cdot 10^3$	4.8	2	1
		$T = 8$	$670 \pm 80$	$57 \pm 6$	$1.86 \cdot 10^3$	5.6		
		$T = 10$	$960 \pm 130$	$82 \pm 10$	$2.67 \cdot 10^3$	8.1		

a) The width may be either the width of a coherent resonance state or the width of a discrete state.

$$b) R = E_x^x \cdot B(E_x)/EWSR(E_x, AT) \cdot 100$$

TABLE 6. Compilation of all the results from this experiment.

taken and fitted with 10 data points per MeV. For graphical purposes the number of points for the 90° spectra was reduced in the continuum range by a factor of 4, the 120° spectra by a factor of 2. The fitting range was 5-45 MeV, the broken lines are drawn to guide the eye. The error for the 90° data is of the size of the data points.

**FIGURE 4** 92.5 MeV electrons scattered inelastically from  $^{89}\text{Y}$  at 75°, 90°, 105° and 120°. The fitted background (consisting of radiation tail, "target-in," and "target-out" background), as described in the text has been subtracted. The relative change in peakheight of the single resonances, used and needed to decompose the cross section into its components, indicates very clearly the various multipoles contributing. Note that the cross sections fall off more than an order of magnitude between 75° and 120°. Apparent differences to Figures 2, 3 and 7 are due to correction for the constant dispersion of the magnetic spectrometer which has been applied in this Figure but not in the others and to the subtraction of the ghost peak around 7.5 MeV.

6  
v1

The Goldhaber-Teller model fits both the results of this work and the photon point from Refs. 22 and 23, while the Steinwedel-Jensen model, if fitted to the (e,e') data, misses the photon point by a factor of 2. An E2 (or E0) assignment of the cross section at 17 MeV can clearly be ruled out; as upper limit 5% of the isoscalar E2 sum rule (or 10% of the isoscalar E0 sum rule) may be estimated.

**FIGURE 5** Spectrum of 92.5 MeV electrons scattered inelastically at 90° from  $^{89}\text{Y}$ . The T, E1 state is more clearly visible with this extended scale than in the 90° data of Figure 3 or 4. The cross sections have been corrected for the constant momentum dispersion of the spectrometer.

**FIGURE 6** Similar to Figure 3, but for 105° and a fitting range of 5-40 MeV. The data are those of Figure 2. The broken lines at 17 MeV indicates the height 100% of the monopole sum rule, as proposed by Ref. 8, would have in a resonance 4 MeV wide and how the composite cross sections would look.

**FIGURE 7** Relative DWBA cross section, calculated using the Goldhaber-Teller model, as fitted to the experimental cross sections for the resonance at 14 MeV

**FIGURE 8** Comparison of relative DWBA and experimental cross sections for the resonance found at 16.6 MeV.

with a width of  $\Gamma = 4.5$  MeV. The comparison rules out any assignment other than E2.

**FIGURE 9**  
Relative DWBA cross section using the Goldhaber-Teller model as compared to the resonance at 28 MeV assuming a width of  $\Gamma = 8$  MeV. The comparison shows that the cross section in this region is predominantly E2 with the possibility of some E3 contribution.

Relative DWBA cross section calculated with the Goldhaber-Teller model for the structure at 13.5 MeV with a width of 1.2 MeV. Comparison with experiment favors an E3 assignment. M2 assignment would be possible, too, but was not considered seriously possible, due to the great M2 strength necessary to explain the data.

**FIGURE 11**  
Relative DWBA cross section using the Goldhaber-Teller model as compared to the cluster of states concentrated around 7 and 8 MeV. The comparison favors an E3 assignment for these states. The large error at the lower momentum transfer is due to the subtraction of the ghost peak.

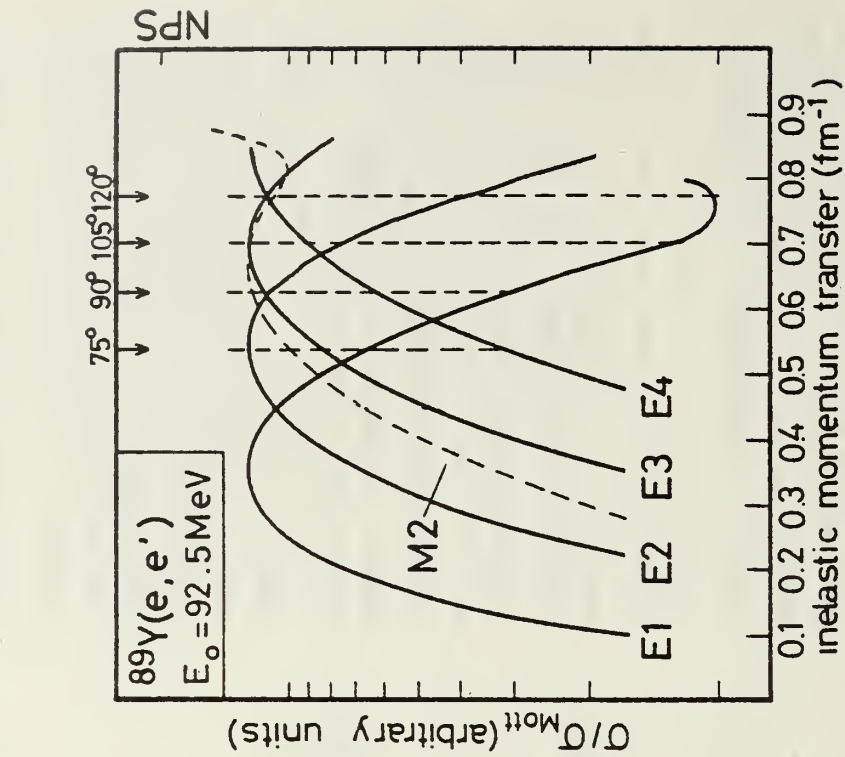


**FIGURE 1**

FIGURE 3 EXCITATION ENERGY (MeV)

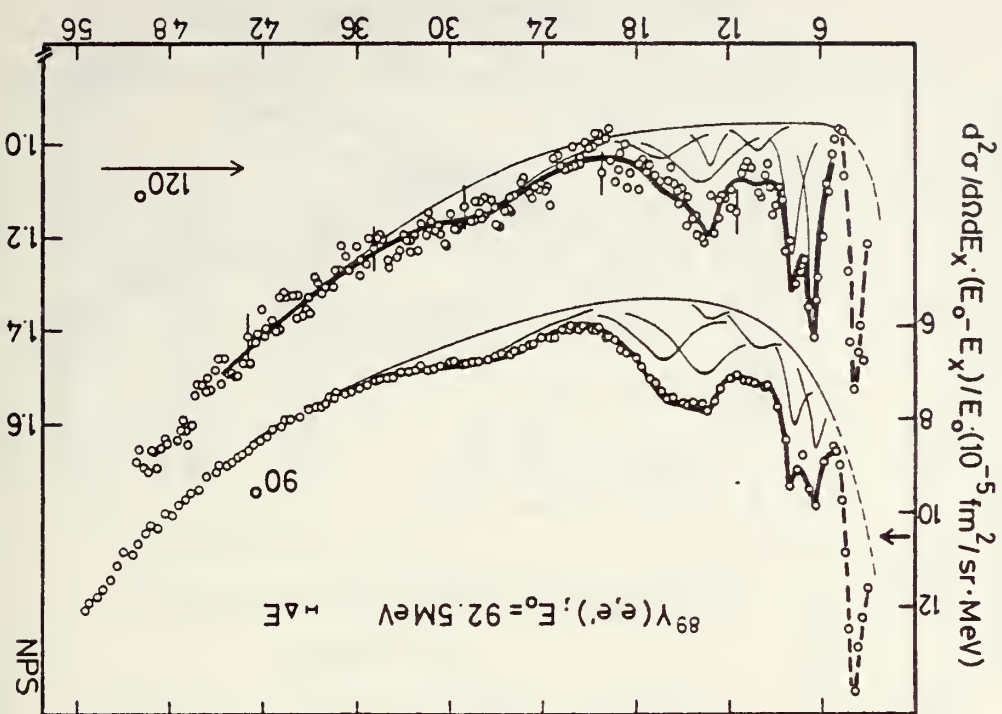


FIGURE 2

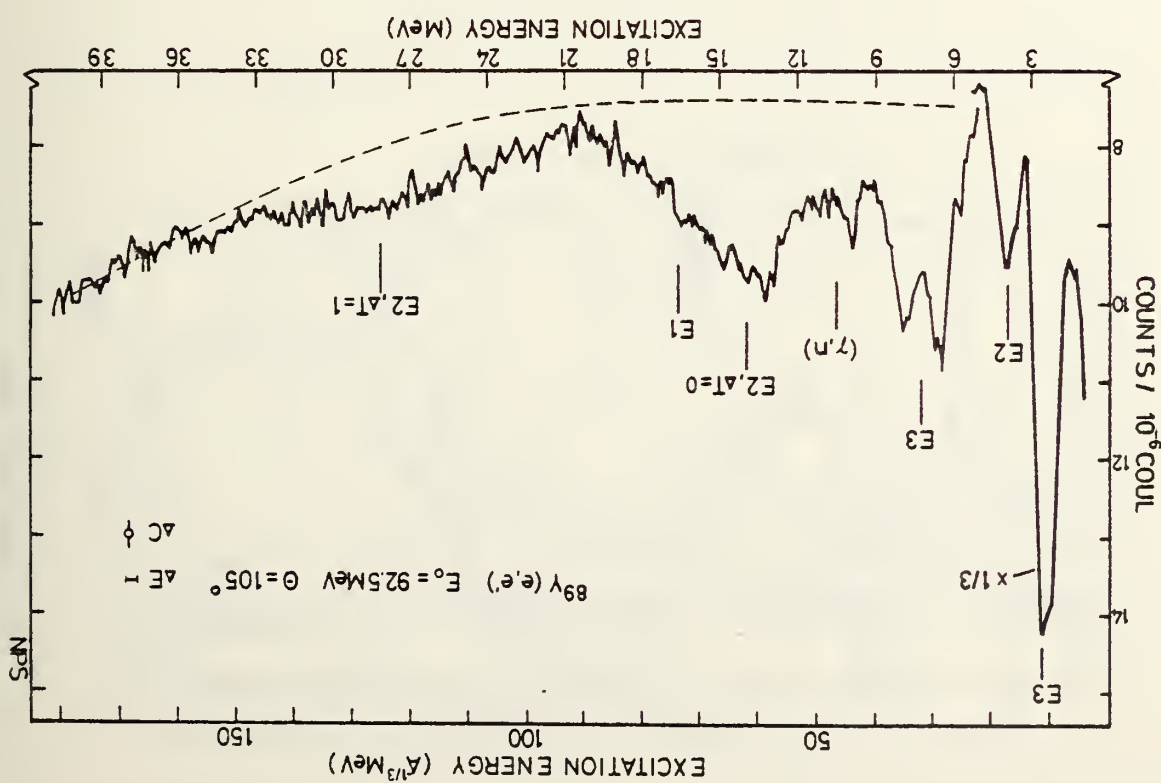


FIGURE 5

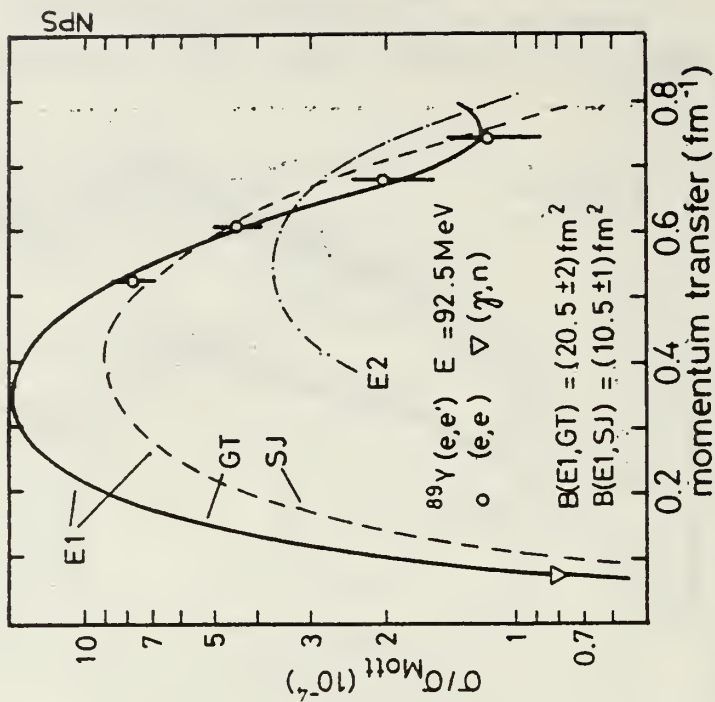


FIGURE 4

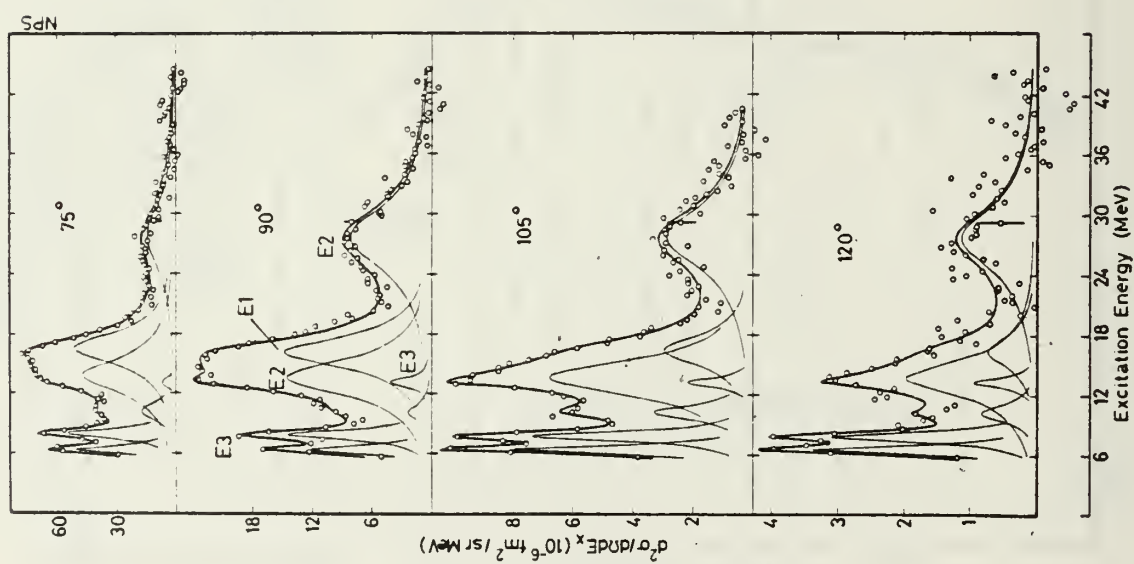


FIGURE 7

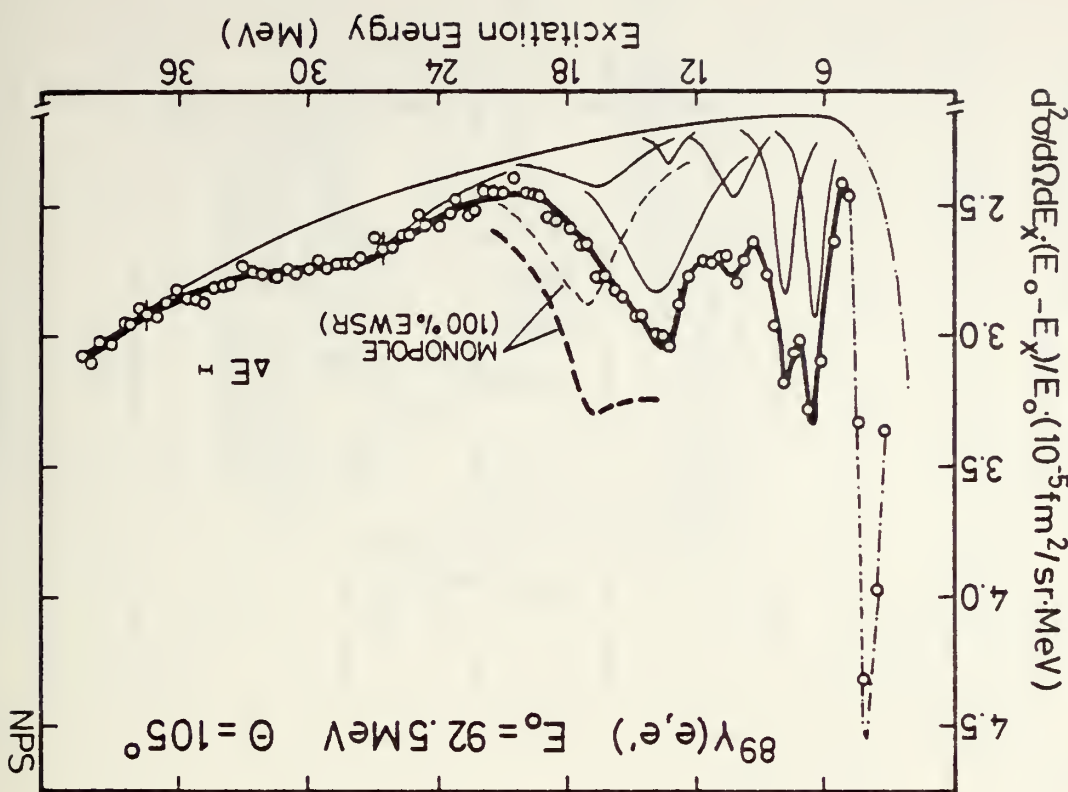


FIGURE 6

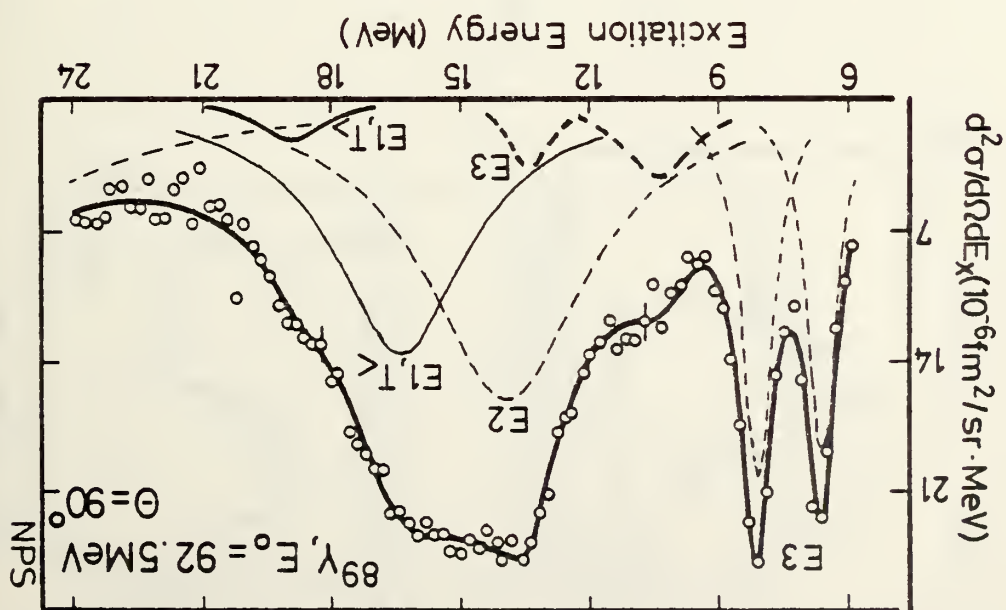


FIGURE 8

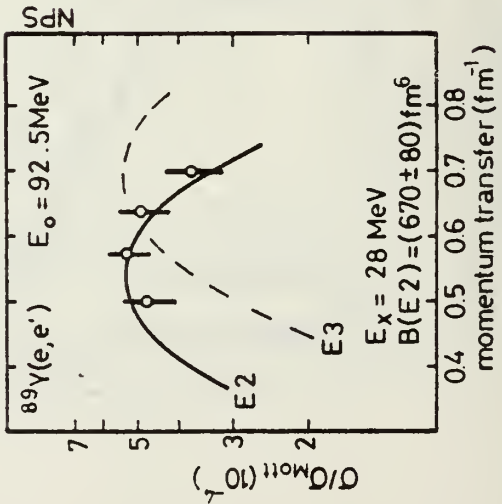
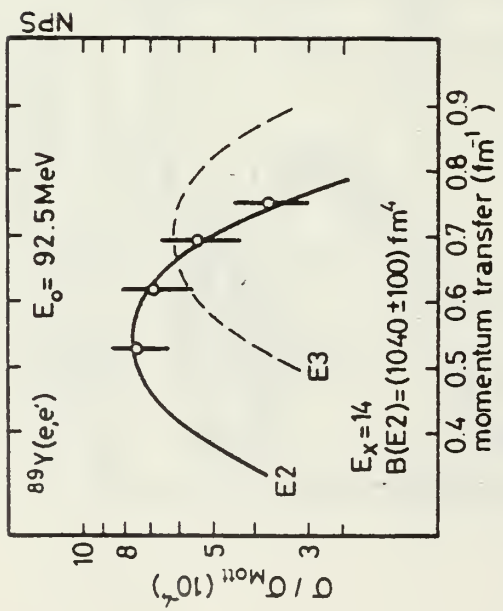
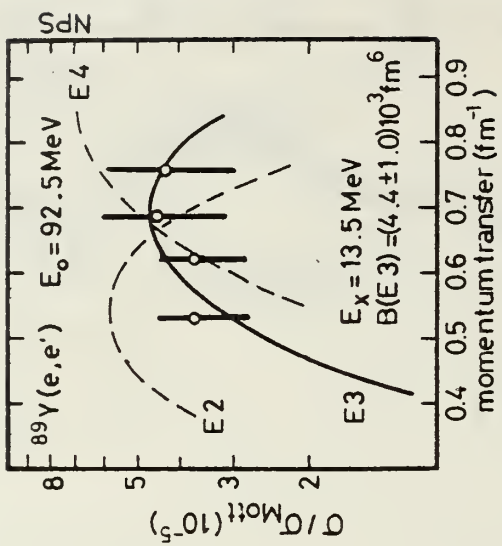


FIGURE 9

FIGURE 10



REFERENCES

1. A. Bohr and B. R. Mottelson, Nuclear Structure, Vol. 2 (Benjamin, Reading, Mass., 1975).
2. R. Pittman and Th. Walcher, Phys. Lett. 36B, 563 (1971).
3. R. Pittman, F. R. Buskirk, E. B. Dally, J. N. Dyer and X. K. Maruyama, Phys. Rev. Lett. 33, 849 (1974) and Phys. Rev. Lett. 34, 848 (1975).
4. R. Pittman and Th. Walcher, Z. Naturforsch. 27a, 1683 (1972).
5. S. Fukuda and Y. Torizuka, Phys. Rev. Lett. 29, 1109 (1972).
6. D. H. Youngblood, J. M. Moss, C. M. Rozsa, J. D. Bronson, A. D. Bacher and D. R. Brown, Phys. Rev. C13, 994 (1976).
7. P. Paul, in "Proceedings of the International Symposium on Highly Excited States in Nuclei," eds. A. Faessler, C. Mayer-Böricken, and P. Turek, Vol. 2 (Jülich 1975).
8. S. Fukuda and Y. Torizuka, Phys. Lett. 62B, 146 (1976).
9. N. Marty, M. Morlet, A. Willis, V. Comparat and R. Frascaria, Preprint, Orsay - PHN - 76 - 03.
10. K. L. Brown, Advances in Particle Physics 1, 71 (1967).
11. C. R. Fischer and G. H. Rawitscher, Phys. Rev. 135B, 377 (1964).
12. H. A. Bentz, R. Engfer and W. Bühring, Nucl. Phys. A101, 527 (1967).
13. S. P. Fivozinski, S. Penner, J. W. Lightbody and D. Blum, Phys. Rev. C9, 1533 (1974).
14. L. C. Maximon, Rev. Mod. Phys. 41, 193 (1969).
15. F. R. Buskirk and R. Pittman, Bull. Am. Phys. Soc. 21, 683 (1976), and to be published.

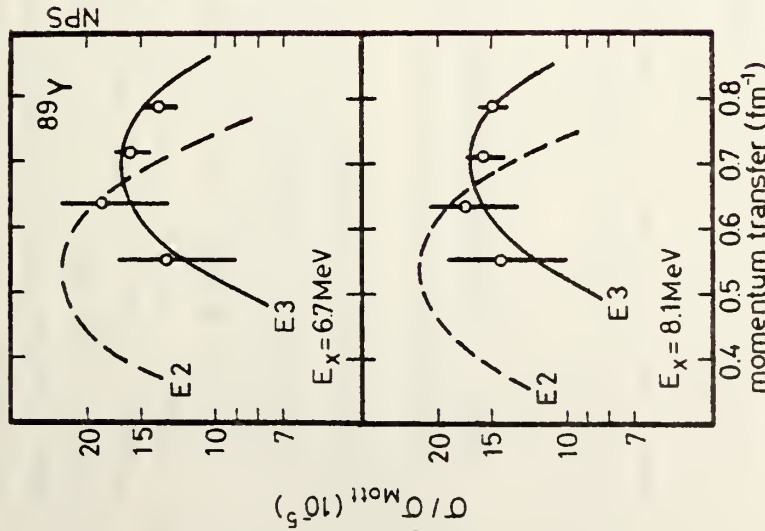


FIGURE 11

16. R. Pitthan, *Z. Physik* 260, 283 (1973).
17. E. F. Gordon, M. S. Thesis, Naval Postgraduate School, 1975 (unpublished); E. F. Gordon, F. R. Buskirk and R. Pitthan, to be published.
18. J. F. Ziegler and G. A. Peterson, *Phys. Rev.* 165, 1337 (1968).
19. S. J. Skorka, J. Hertel and T. W. Reetz-Schmidt, *Nucl. Data A2*, 347 (1966).
20. J. Weneser and E. K. Warburton, in "The Role of Isospin in Nuclear Physics," edited by D. H. Wilkinson (North-Holland, Amsterdam, 1969).
21. R. A. Ferrell, *Phys. Rev.* 107, 1631 (1957).
22. B. L. Berman, J. T. Caldwell, R. R. Harvey, M. A. Kelly, R. L. Bramblett, and S. C. Fultz, *Phys. Rev.* 162, 1099 (1967).
23. A. Leprêtre, H. Beil, R. Bergère, P. Carlos, A. Veyssiére, and M. Sugawara, *Nucl. Phys.* A175, 609 (1971).
24. D. B. Isabelle and G. R. Bishop, *Nucl. Phys.* 45, 209 (1963).
25. S. Tuan, L. E. Wright, D. S. Onley, *Nucl. Instr. Meth.* 60, 70 (1968).
26. L. J. Tassie, *Australian J. Phys.* 2, 407 (1956).
27. A. Migdal, *J. Phys. USSR* 8, 331 (1944); M. Goldhaber and E. Teller, *Phys. Rev.* 74, 1046 (1948).
28. H. Steinwedel and H. Jensen, *Z. Naturforsch.* 5a, 413 (1950).
29. S. Fallieros and B. Gouard, *Nucl. Phys.* A147, 593 (1970).
30. P. Paul, in "Proceedings of the International Conference on Photonuclear Reactions and Applications," Asilomar, 1973, edited by B. L. Berman (Lawrence Livermore Laboratory, Univ. of California, Livermore, 1973).
31. Y. Kawazoe, Res. Rep. Lab. Nuclear Science, Tohoku University 6, 211 (1973).
32. B. R. Mottelson, *Science* 193, 287 (1976); *Reviews of Modern Physics* 48, 375 (1976); and *Fysisk Tidsskrift* 74, 97 (1976).
33. S. S. Hanna, preprint 1977.
34. B. R. Mottelson, in "Int. Conf. on Nucl. Structure," Kingston 1960, eds. D. A. Bromley and E. W. Vogt (Univ. of Toronto Press and North-Holland, Amsterdam, 1960); A. Bohr, in "Int. Nucl. Physics Conf.," Gatlinburg 1966, eds. R. Becker, C. Goodman, P. Stelson and A. Zucker (Academic Press, New York, 1967).
35. S. Krewald and J. Speth, *Phys. Lett.* 52B, 295 (1974); I. N. Borzov and S. P. Kamerdzhiev, *Sov. J. Nucl. Phys.* 21, 15 (1975).
36. A. Kiss, C. Mayer-Börücke, M. Rogge, P. Turek and S. Wiktor, *Phys. Rev. Lett.* 37, 1188 (1976).
37. N. Auernbach and A. Yeverechyahu, *Ann. Phys. (N.Y.)* 95, 35 (1975).
38. N. Auernbach and A. Yeverechyahu, *Phys. Lett.* 62B, 143 (1975).
39. G. L. Moore, F. R. Buskirk, E. B. Dally, J. N. Dyer, X. K. Maruyama and R. Pittman, *Z. Naturforsch.* 31a, 668 (1976).
40. N. Marty, M. Morlet, A. Willis, V. Comparat, R. Frascaria, *Nucl. Phys.* A238, 93 (1975).
41. J. M. Moss, C. M. Rosza, J. D. Bronson and D. H. Youngblood, *Phys. Lett.* 53B, 51 (1974).
42. A. Schwiercinski, R. Frey, E. Spamer, H. Theissen and Th. Walcher, *Phys. Lett.* 55B, 171 (1974).

43. F. S. Dietrich, D. W. Heikkinen, K. A. Snover, and K. Ebisawa, *Phys. Rev. Lett.* 38, 156 (1977).
44. H. Überall, *Electron Scattering from Complex Nuclei* (Academic, New York, 1971).
45. I. Hamamoto, in "Proc. of the Int. Conf. on Nuclear Structure Studies Using Electron Scattering and Photoreaction," Sendai, 1972; eds. K. Shoda and H. Uji (*Suppl. Res. Rep. Lab. Nucl. Sci., Tohoku Univ.*, Vol. 5, 1972).
46. W. A. Houk, R. W. Moore, F. R. Buskirk, J. N. Dyer and R. Pitthan, *Bull. Am. Phys. Soc.* Vol 22, No. 4 (Washington Meeting).
47. J. M. Moss, D. H. Youngblood, C. M. Rozsa, D. R. Brown and J. D. Bronson, *Phys. Rev. Lett.* 37, 816 (1976).

## Distribution List

	No. Copies
1. Library Code 0212 Naval Postgraduate School Monterey, CA 93940	2
2. Dean of Research Naval Postgraduate School Monterey, CA 93940	2
3. Professor Fred Buskirk Department of Physics and Chemistry Naval Postgraduate School Monterey, CA 93940	2
4. Dr. Rainer Pitthan Department of Physics and Chemistry Naval Postgraduate School Monterey, CA 93940	2
5. Professor K. E. Woehler Chairman Department of Physics and Chemistry Naval Postgraduate School Monterey, CA 93940	1
6. National Science Foundation Division of Grants and Contracts Washington, D.C. 20550	2
7. Dr. William Rodney National Science Foundation Washington, D.C. 20550	1

U178577

DUDLEY KNOX LIBRARY - RESEARCH REPORTS



5 6853 01071308 4

U17857